universität wien

DIPLOMARBEIT / DIPLOMA THESIS

Titel der Diplomarbeit / Title of the Diploma Thesis

„Photoswitchable Monoamine Transporter Ligands in the human Serotonin Transporter"

verfasst von / submitted by

Sophia Schnabl

angestrebter akademischer Grad / in partial fulfilment of the requirements for the degree of

Magistra der Pharmazie (Mag.pharm.)

Wien, 2017 / Vienna, 2017

Studienkennzahl lt. Studienblatt / degree programme code as it appears on the student record sheet	A 449
Studienrichtung lt. Studienblatt / degree programme as it appears on the student record sheet	Diplomstudium Pharmazie
Betreut von / Supervisor:	Univ.-Prof. Mag. Dr. Gerhard F. Ecker
Mitbetreut von / co-Supervisor:	Mag. Dr. Lars Richter

Acknowledgements

Working on my diploma thesis was the most exciting and most challenging experience in my University career. I met a lot of people who helped me to do my first steps in scientific research.

Foremost, I want to thank Prof. Dr. Gerhard Ecker for giving me the opportunity to take the first insights of doing scientific research under his supervision. Although working in the pharmacoinformatic field was a new experience for me, he always showed confidence, that I would manage it easily. The project assigned to me was a current topic in pharmaceutical research and included a collaboration with a group on the TU Vienna. I want to thank you for the profound insight into the world of pharmaceutical science beyond the study of pharmacy, particularly with the opportunity to present my scientific results in a poster session at a congress in Schladming.

My biggest thanks go to Mag. Eva Hellsberg for enlightening my first glance on scientific research. Eva offered me systematic guidance in the scientific field and training in the different scientific tools. Even though, Eva was engaged in her own PhD research, besides preparing conferences and speeches, she invested countless hours in fruitful discussions on my work and results. Her excellent networking skills encouraged me to improve my own soft skills as well. I cannot thank you enough for your tremendous support. Thank you for all the motivation and always finding the right words.

Special thanks I want to give to Dr. Lars Richter, who improved my scientific thinking. Lars challenged my results over and over again with precisely the questions to drive my project forward. Thank you for always being encouraging.

Working on my thesis, I was integrated in an international research group and I want to thank everyone in this team for their continuous support. Our scientific discussions were extremely constructive for my project and enhanced my English skills. We always had a lot of fun together and I enjoyed working with you.

Last but not the least, I would like to thank my family: my parents and my two sisters for being curious about my research, for supporting me with pride and sharing my enthusiasm.

Table of contents

1 Introduction

Drug development covers research for new active substances with new modes of actions and improvement of existing pharmaceuticals. Drug development begins with understanding of both regular and pathologic processes in biological systems. The knowledge of coherences in the human body implicates the possibility to create drugs which show fewer side effects. If there is for instance a lack of an endogenous substance responsible for an illness, scientists try to find a way to increase the blood level of this substance. There are several approaches like the supply of the lacking substance or its precursor or the stimulation of the specific cells, which generate this substance. Another strategy would be to block the transporters, which carry the substance in question into cells or to limit the metabolising factors responsible for the substance.

While in former days the only way to examine efficacy and side effects was to test substances in biological systems, nowadays scientists search for possible effective drug molecules with the help of computational methods, called *in silico* (from Latin "in silicon", referring to the usage of silicon for computer chips) (World Wide Words: In Silico, 2017). Large virtual libraries are available containing possibly active molecules. For better comprehension of the behaviour of molecules in a biological system, researchers work with computational algorithms based on physical molecular mechanics. So-called molecular modelling methods predict amongst others electrostatic atom interactions, poses and behaviours of proteins or drug components (Leach, 2001).

1.1 Serotonin and the human Serotonin Transporter

Serotonin (5-hydroxytryptamine) is one of the most important neurotransmitters in mammalians. It received its name due to its impact on the blood pressure: belonging to the components of the serum, serotonin regulates the tone on blood vessels. Moreover, serotonin acts on the activity of the gastrointestinal motility and stimulates the central nervous system. It is generally known to affect feelings like happiness. In fact, serotonin regulates mood, sleep, pain, appetite and body temperature (Sauermost et al., 1999).

Serotonin is transported by specific proteins, called human serotonin transporters. These proteins have a high affinity binding site for serotonin.

1.1.1 Transport Mechanism

The serotonin transporter (5-hydroxytryptamine-transporter, 5-HTT) is prevalent in most of the fauna. Homologies of the human serotonin transporter can be found in very primitive animals and even in prokaryotes. hSERT belongs to the family of monoamine transporters together with the norepinephrine transporter (NET) and the dopamine transporter (DAT) (Ramamoorthy et al., 2011).

With the power of the Na^+-/K^+-ATPase serotonin and sodium get transported into the neural cell, whereas potassium leaves the cell. This mechanism depends on the concentration of the ions and implicates a conformational change of such a sodium transporter system. The exact mechanism is not fully understood until now, but schematically shown in Fig. 1.

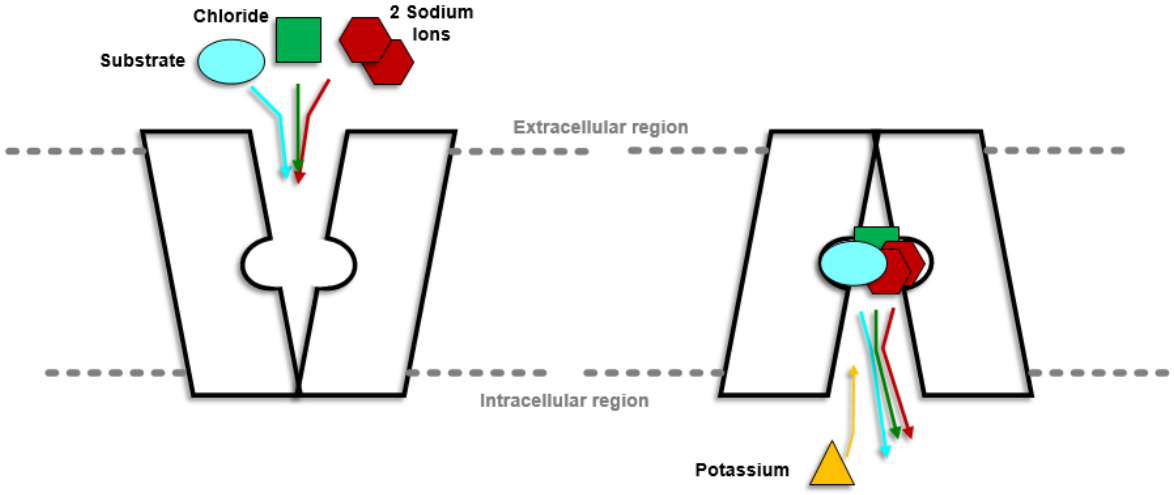

Fig. 1 - A schematic illustration of the transport mechanism of a sodium-symporter. In the *outward-facing open* conformation (left) the substrate molecule, two sodium ions and a chloride ion enter the binding site of the transporter protein. The substrate's binding to the transporter concludes in a conformational change of the transporter protein. When the *inward-facing open* conformation (right) is adapted, the substrate molecule and the ions are released into the cytoplasm, while in case of SERT a counter ion (potassium) binds to the transporter protein. (image adapted from Kristensen et al., 2011)

The human serotonin transporter is responsible for eliminating free serotonin from the extracellular region, the synaptic cleft (Fig. 2), and thereby down-regulates the neurotransmitter's impacts on the body.

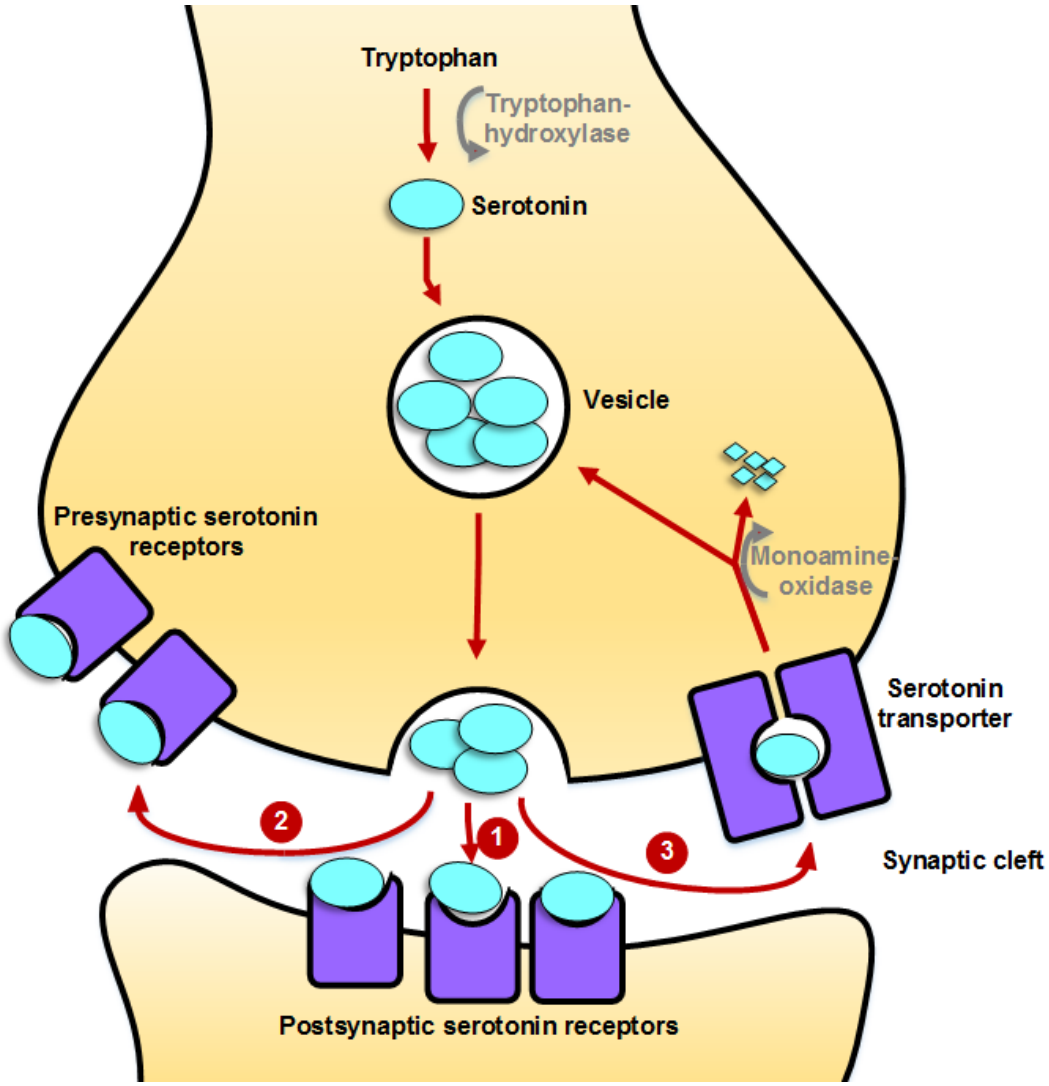

Fig. 2 – The serotonin synapse. Tryptophan is changed into serotonin by the enzyme tryptophan hydroxylase and then packed into vesicles. These are transported to the synaptic cleft, where serotonin is released from the neuron when stimulation occurs. Serotonin shows three actions. (1) It binds to its postsynaptic receptors on the opposite neuron where the signal is transferred to the following neurons. (2) It binds to the presynaptic serotonin receptors on the neuron it comes from as well. There it is responsible for giving feedback for the regulation of the presynaptic neuron's plasticity. (3) Presynaptic hSERTs take back in the free serotonin which is then recycled for reuse or broken down for excretion in urine. (Image adapted from Rot et al., 2009)

1.2 Serotonin Regulating Drugs

A considerable number of pathogenic processes are known to negatively influence the optimal level of serotonin. Mostly, mental stress and depressions are observed in patients with too low serotonin levels in brain liquor, whereas too high concentrations of the neurotransmitter may cause anxiety within patients (Boyer, 2016).

Thus, clinical research focused on identification of drugs to control and balance the serotonin level in the body. Meanwhile, there are several drugs on the market which competitively block hSERT and thus regulate the blood serotonin level.

Today's research focuses on mood regulator drugs and antidepressants with different modes of action. In 1958, the first antidepressant drug, Imipramine, got available on the market (U.S. Food and Drug Administration, 2017). It belonged to the group of monoamine oxidase inhibitors (MAOI). Monoamines like serotonin, norepinephrine and dopamine are degraded by the enzyme monoamine oxidase. By inhibition of these enzymes via MAOI drugs, the monoamines' effects are prolonged. Unfortunately, MAOIs not only raise the serotonin level but norepinephrine and dopamine concentrations are influenced too (Wimbiscus et al., 2010). This led to several adverse events.

A different approach to cure depressive disorders are tricyclic antidepressants (TCAs), which are named after their structure. The antidepressive effect is based on the inhibition of degradation of monoamines similar to MAOIs and therefore the same spectrum of adverse events was observed (Pruthi, 2017).

To reduce the negative side effects, research focused on selective serotonin reuptake inhibitors (SSRIs), meanwhile the most common class of antidepressants. The human serotonin transporter became target of several mood elevator drugs and antidepressants. SSRIs are molecules, which selectively inhibit hSERT, so that serotonin molecules are no longer able to bind to the transporter protein. Thus, the neurotransmitter is unable to enter the neural cell. Consequently, the concentration of serotonin increases in the extracellular region. This leads to extended and higher effects of the neurotransmitter and should relieve signs of depression, particularly when the serotonin concentration rises in the brains tissue fluid (Cipriani et al., 2012).

SSRIs are long known to be used against depressive disorders and a considerable number of drugs in this category are on the market for more than 30 years. The first SSRI available in Europe was fluvoxamine in 1983. It came on the market in Austria in

1996 (myHealthbox, 2017). Other common SSRI drugs are paroxetine, citalopram (racemic form, R and S isomer) and sertraline.
With SSRIs, depressive disorders are treated with much less side effects than with other antidepressants because they show a much lower affinity to other monoamine receptors.

1.2.1 Escitalopram

One of the most frequent prescribed SSRI drugs is escitalopram ((S)-citalopram) (Fig. 3), the high affinity enantiomer of citalopram, first-time authorised in 1996. Escitalopram is on the market since 2001 and 2002 in EU and Austria, respectively (myHealthbox, 2017). Regarding interactions with other drugs, citalopram and escitalopram are considered as advantageous in comparison to other SSRI drugs. (Benkert et al., 2016)

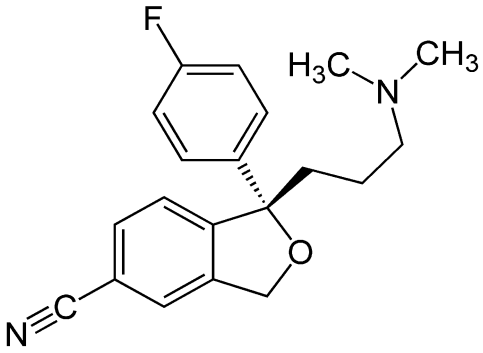

Fig. 3 – Escitalopram, (S)-1-(3-dimethylaminopropyl)-1-(4-fluorophenyl)-1,3-dihydro-2-benzofuran-5-carbonitrile

1.3 hSERT Protein Structure

For understanding the mechanism of how the serotonin transport works, the binding mode of the drug molecule and therefore the molecular structure of the protein have been target of investigations. A technique called homology modelling allows to assume protein structures by creating a model of the requested protein based on the already known amino acid sequence of a similar protein. In case of hSERT, scientists referred to the homology on the bacterial leucine transporter (LeuT) and the *Drosophila melanogaster* dopamine transporter (dDAT) for a long period (Green et al., 2015).

Crystal structure analysis is another approach for more precise evaluation of a protein structure and binding mechanisms. X-rays are used to create a picture of a protein crystal, from which a 3-dimensional structure can be calculated (Smyth et al., 2000). Only a few proteins of the human body were successfully crystallized until now.
The first crystal structure of a transporter, homologous to neurotransmitter transporter, LeuT, was published in 2005 (Yamashita et al., 2005) and more recently a crystal structure of dDAT was analysed (Penmatsa et al., 2013). Since LeuT and dDAT are known to possess homolog structures to other monoamine transporters, scientists used this knowledge to explore hSERT in greater detail.
Coleman et al. successfully crystallized the structure of hSERT in a co-crystallization experiment with hSERT and a known hSERT inhibitor drug, namely escitalopram (Coleman et al., 2016) (Fig. 4). New possibilities for hSERT specific drug research got conceivable.
With this experiment, the structure of hSERT was confirmed. It consists of twelve helices and several binding sites for sodium, chloride and serotonin, respectively, in the outward-facing open state. Furthermore, the two binding sites within hSERT for serotonin or drugs like escitalopram were verified, a central and an allosteric binding site. (Plenge et al., 2012).

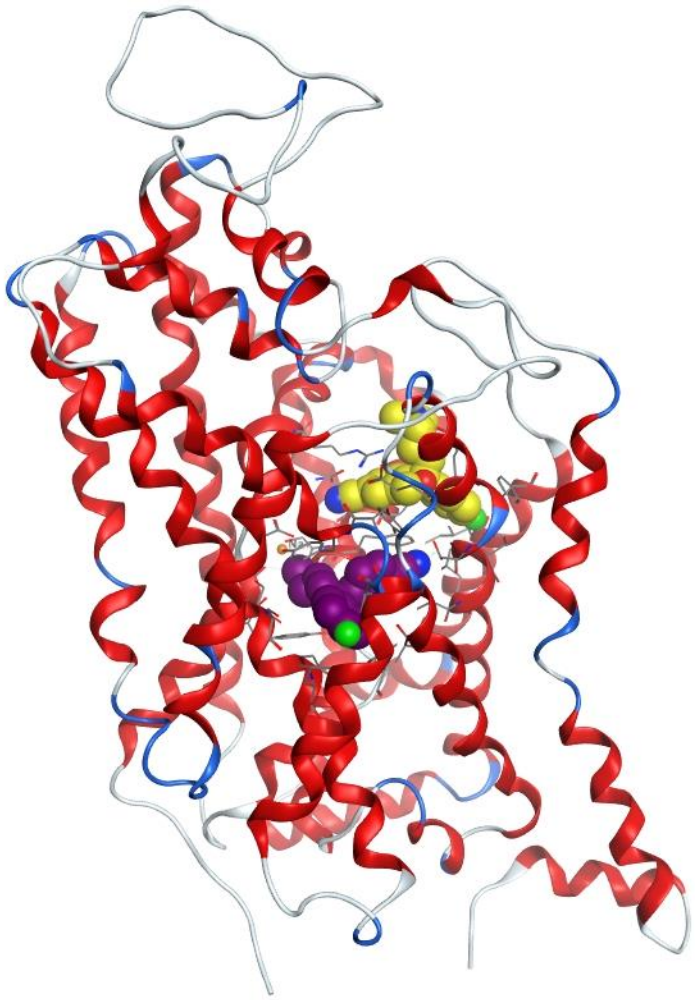

Fig. 4 - Crystal structure of hSERT, PDB 5I73, with two escitalopram molecules bound, one in the allosteric (yellow) and one in the central binding site (violet). Resolution 3.24Å. Visualized in MOE (Coleman et al., 2016)

1.3.1 Central and Allosteric Binding Site

The central binding site of hSERT is also called the orthosteric binding site from greek ὀρθός (*orthós*) meaning right and proper and στερεός (*stereos)* means “solid”. This indicates that this region of the protein is the main binding site for the substrate. Most drugs with the target location on hSERT work competitive, which means they are designed to fit into the central binding site with the effect to compete with serotonin for the occupation of the binding pocket.

The other binding site in hSERT is an allosteric binding site. Allostery derives from the Greek words ἄλλως (*allos)* meaning “other” and στερεός (*stereos)* meaning “solid”. In

general, an allosteric transporter protein can assume two or more stable conformations initiated by enzymes, which do not bind to the main binding site, but to another, an allosteric binding site. By interacting, allosteric modulators can cause a change of conformation of the central binding site and therefore lead to activation (allosteric stimulation or positive allosteric effect) or inhibition (allosteric inhibition or negative allosteric effect) of the transporter molecule (LeVine et al., 2016).

Proteins with an additional allosteric binding site next to the main one are of interest for scientific research concerning new drugs, which can modulate the protein by affecting only the allosteric region. This means, drug molecules would not need to fit into the exact substrate binding pocket, but could be modulators on the allosteric region, which may be easier to approach.

hSERT was found to possess such an allosteric binding site in the extracellular vestibule (Plenge et al., 2012). Studies have shown, that when the allosteric region is occupied by escitalopram, the off-rate of escitalopram bound in the central binding site is slowed down (Coleman et al., 2016). This can be explained by the location of the allosteric site in hSERT, which is positioned above the central site and nearer to the extracellular region, which means, escitalopram has to pass the allosteric binding site in order to reach the central binding site (Fig. 5).

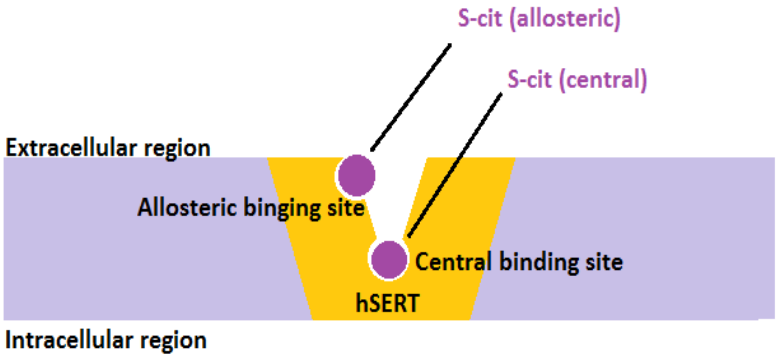

Fig. 5 – Schema of hSERT in the cell membrane. The allosteric binding site is located “above” the central binding site. When exiting the transporter protein, escitalopram in the central binding site (S-cit (central)) passes the allosteric binding site. When latter is occupied by a second escitalopram molecule (S-cit (allosteric)), S-cit (central) cannot pass. It therefore has to wait until S-cit (allosteric) dissociates and reveals the path. This explains the delay of dissociation of a escitalopram molecule in the central binding site upon presence of a second escitalopram molecule in the allosteric binding site.

1.3.2 Extracellular Gate

Former studies found out, that the two aromatic amino acids tyrosine (Tyr176) and phenylalanine (Phe335) function as lid between the two binding pockets of hSERT (Gabrielsen et al., 2012). Their aromatic side chains are able to flip (Fig. 6), blocking the transport of molecules between the two binding sites. Phe335 is more flexible than Tyr176, it switches between conformations by 90° difference. In some experiments the inhibitor molecules got stuck between these two amino acids, preventing the closure of the gate. Furthermore, study results suggest, that the inhibitor molecules interacted with amino acid side chains in both binding sites at the same time. Consequently, the transporter protein is no longer able to close the extracellular gate and therefore cannot change its conformation to an inward-open protein. These findings conclude in a possible explanation for a mechanism of hSERT inhibition.

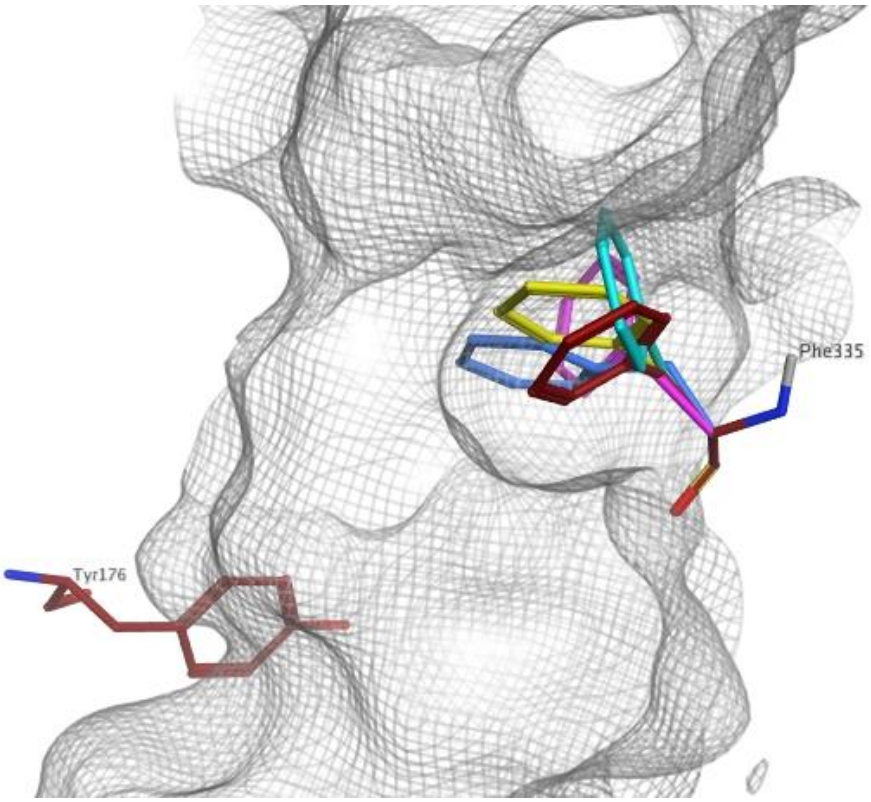

Fig. 6 – Tyr176 and Phe335 are located between the two binding pockets of hSERT and their side chains' high flexibility leads to their function as a lid, preventing the closure of the extracellular gate. Visualized in MOE, showing different rotamers of Phe335 gathered in our docking studies.

1.4 Photopharmacology

Already in the 19th century first photochromatic compounds were found (te Meer, 1876). Photochromy from Greek φωτός (photos = light) and Χρώμα (chroma = color) is a physical characteristic describing light induced change of molecules into another conformation. This process is reversible and results in a change of physical properties, for example a different absorption spectrum. In photopharmacology this induced conformation change is used to turn a molecule from an inactive configuration into an active one.
First, only inorganic substances were used; for instance, in erasable optical memory media. Upon development of the CD-R (compact disk-recordable), organic materials found their way into practice (Irie, 2000).

Three criteria are necessary to work with photoswitchable molecules: the two conformation states

- must have different physical and chemical properties,
- must be thermally stable and
- must be separately addressable (Katsonis et al., 2007).

The difference of chemical properties for photoswitchability is based on conformation and configuration of a molecule.
The conformation of an organic molecule describes the 3-dimensional arrangement of the C-atoms, like their 3D-coordinates. Molecules which distinguish only in rotation around a single bond are called isomers, rotamers or conformers. They can convert into each other by overcoming a certain amount of energy barrier.
Configuration, on the other hand, is defined as 3-dimensional arrangement of a molecule's atoms without consideration of rotation around single bonds. Two isomers, which distinguish in their configuration, cannot be superposed by rotation around single bonds. The heavier substituent on each site of the containing double bond defines the configuration. If they both lie on the same side, "above", the double bond, the structure is called Z-isomer, if the lie on different sides, one "above", the other one "beneath" the double bond, the molecule is an E-isomer. Configurational isomers distinguish in their chemical and physical properties, which is an important fact when examining drug molecules.

According to the Cahn–Ingold–Prelog (CIP) sequence rules each atom connected to the stereo centre arranged is labelled in decreasing order according to the atomic number. The lowest number is pointed towards the viewer. If the numbers of the remaining atoms decrease in the right direction, clockwise, the configuration of the molecule is labelled R for rectus (Latin), or counter clockwise S for sinister (Latin). (Cross et al., 1974) In this diploma thesis we work with (S)-citalopram, which cannot be superposed with (R)-citalopram and is advantageous concerning its effects on the human body.

The rather new research topic photopharmacology deals with drug molecules which switch from their inactive configuration to the active one by stimulation with light. These changes are reversible. The idea behind photoswitchable drugs is to distribute the inactivated substance in the organism and then activate the molecules only at the target location. Furthermore, the exact timing of activation and an accurate duration could be triggered. This is considered to improve the efficacy of the drug and to reduce the side effects. (Gómez-Santacana et al., 2017)
Until now only a few structures are known, which can be stimulated to a configurational change by light. In this diploma thesis, the focus will be laid on compounds containing a diazo-bond (Fig. 7) or a hemithioindigo structure (HTI) (Fig. 8). These compounds are known to change their configuration when stimulated by light. Drug molecules like escitalopram, chemically altered with azo- and/or HTI-groups, have been the target of investigation regarding the efficacy and activity of such drugs.

1.4.1 Azo-Compounds

Structures containing diazo-bonds may change their configuration under impact of light. (Fig. 7) (Irie, 2000) Their basic state is in E-configuration, in which they are relaxed and more stable. According to some experimental data (see 3. Table 1), the activity values of azo-compounds are lower when in E-configuration indicating that these compounds should fit better into hSERT than azo-compounds in Z-configuration.

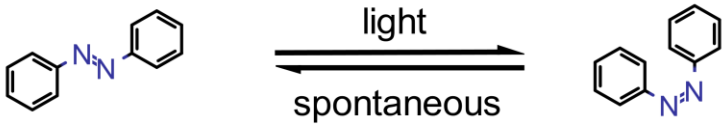

Fig. 7 – (E)-diphenyldiazene (left) switching to (Z)-diphenyldiazene (right).

1.4.2 Hemithioindigo-Compounds

Hemithioindigo structures are unsymmetrical, containing a thioindigo part linked to a stilbene fragment via central double bound (Fig. 8). (Wiedbrauk et al., 2015) The Z-configuration is the thermodynamically stable basic state, which can be photoisomerized into the metastable E-configuration.

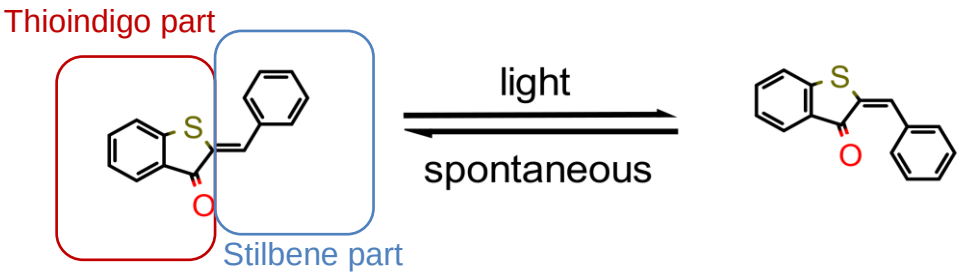

Fig. 8 - (2E)-2-Benzylidene-1-benzothiophen-3(2H)-one (right) switching to (2Z)-2-Benzylidene-1-benzothiophen-3(2H)-one (left). The thioindigo part and the stilbene part are labelled red and blue, respectively, in the schema of the E-configuration.

2 Aim of this Diploma Thesis

Activity of ligands within a protein can be measured *in vitro* or *in vivo* and calculated *in silico*. Benefits of experimenting *in silico* are the repeatable starting conditions, the stable working conditions and thus hopefully recurring results. These parameters are not given to the same extent when working *in vitro*. In this diploma thesis, computational experiments were performed to narrow down the positional options for photoswitchable ligands in hSERT. The research question comprises the differences between Z- and E-configurations in the central binding site. The aim of this diploma thesis was to investigate, whether a photoswitchable compound exists, which fits into the central binding site of hSERT only in one of its configurations. To collect this information, several *in silico* methods were performed, like binding energy calculations, docking studies and common scaffold clustering.

The work is based upon the crystallized structure of hSERT, published by Coleman et al. (2016) and provided by the Protein Data Bank (PDB), a worldwide archive of structural data of biological macromolecules (Berman et al. 2000). The structure's PDB ID is 5I73 and has a resolution of 3,24 Å. It gives an idea how escitalopram binds to the transporter and thus blocks the access for serotonin. To achieve further insight into the binding process, protein-ligand interactions were investigated, binding energies between hSERT and several photoswitchable compounds were calculated and activity values of these ligands were explored. These structures contained an escitalopram scaffold and different photoswitchable substituents, azo- and HTI-fragments (Fig. 9).

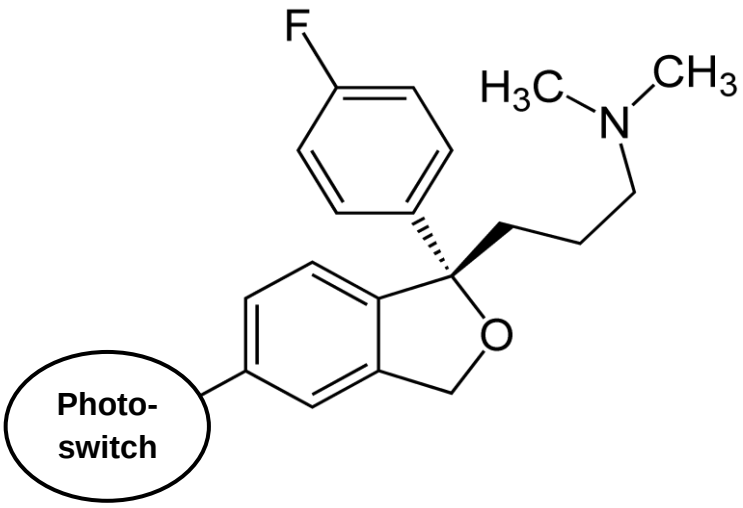

Fig. 9 – Schematic position of the azo- or HTI-structure, labelled as photoswitch on an escitalopram-like scaffold.

The discovery of a compound with a binding energy to hSERT differing markedly whether in E- or in Z-configuration respectively could lead to development of new, light dependent, SSRI drugs.

3 Methods

This work is based upon the crystal structure of the human serotonin transporter, in which two escitalopram molecules are bound, one in the central, the other in an allosteric binding site (Coleman et al., 2016), the PDB ID is 5I73. The focus was set on the central binding site. Therefore, a new pdb-file without the allosteric escitalopram molecule was created. The remaining escitalopram molecule was adapted by substitution of a photoswitchable fragment instead of the cyano-group of escitalopram. Several *in silico* methods, commonly used in pharmacoinformatic research, supported the investigations of the binding mode of the new build compounds, which are based on three structures, Scaffold1 (S1), Scaffold2 (S2), Scaffold3 (S3) (Fig. 10), and are listed in the table below (Table 1).

S1 =

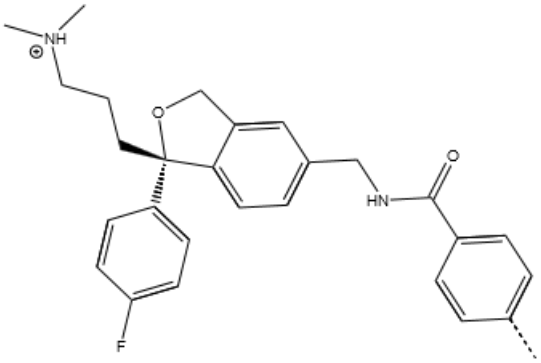

S2 =

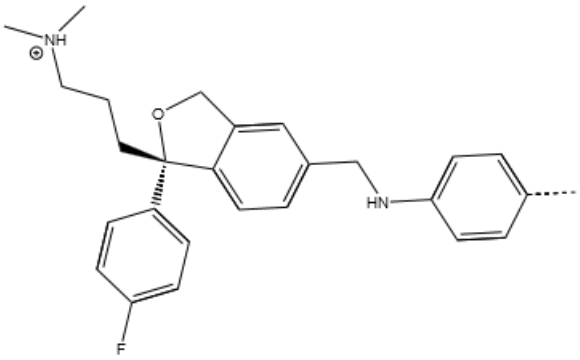

S3 =

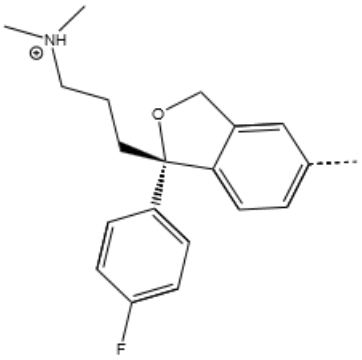

Fig. 10 - Base structures of the tested compounds

Compound	Structure	IC_{50} in hSERT [µM], date of measurement
Escitalopram	S3----C≡N	0.023 2016-10-11
DD-261 azo-compound	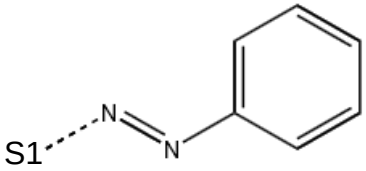	0.594
DD-300 azo-compound	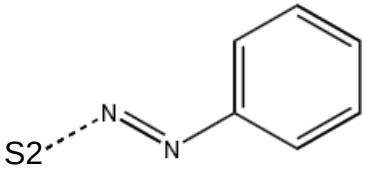	n.d.
DD-301 azo-compound	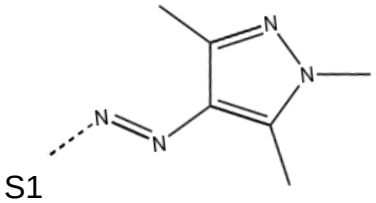	0.462
DD-321 azo-compound	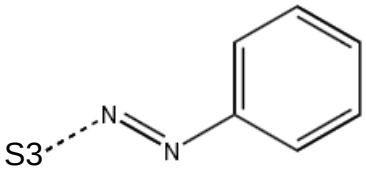	1.049
DD-400 azo-compound	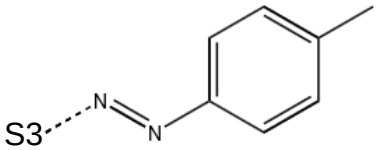	n.d.
DD-402 azo-compound	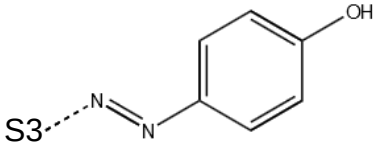	n.d.
DD-403 azo-compound	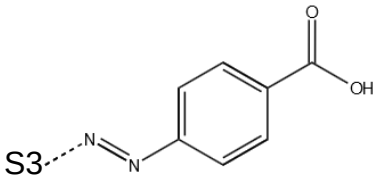	n.d.
DD-405 azo-compound	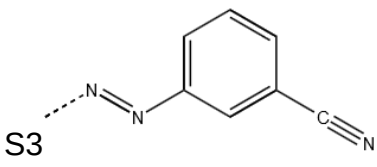	n.d.

Compound	Structure	IC_{50} in hSERT [µM], date of measurement
DD-406 azo-compound	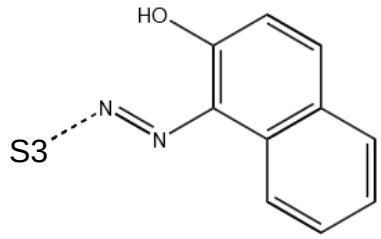	n.d.
DD-355 HTI	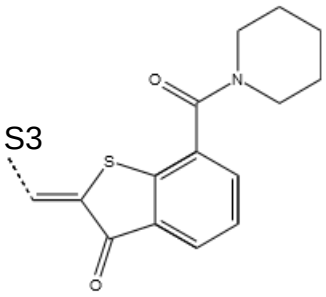	0.418 2016-11-11 0.343 2016-11-11
DD-359 HTI	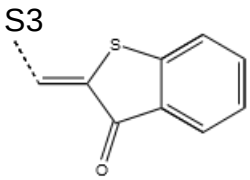	0.149 2016-10-13
DD-355_p HTI	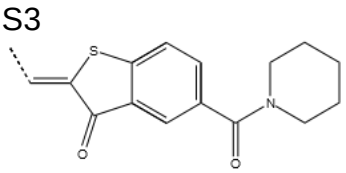	n.d.
DD-355_m1 HTI	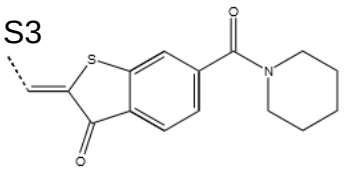	n.d.
DD-355_m2 HTI	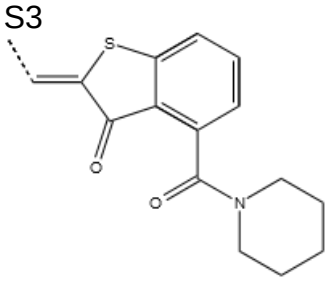	n.d.
DD-350 HTI	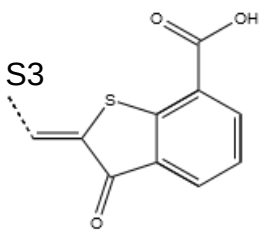	0.377 2016-07-28

Compound	Structure	IC_{50} in hSERT [µM], date of measurement
DD-350^{-} HTI	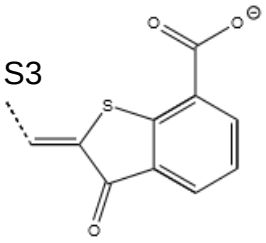	n.d.
DD-353 HTI	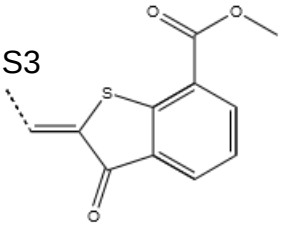	3.363 2016-08-26 1.51 2016-10-13
DD-354 HTI	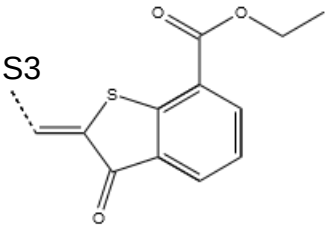	3.789 2016-08-26 1.765 2016-10-13
DD-354_p HTI	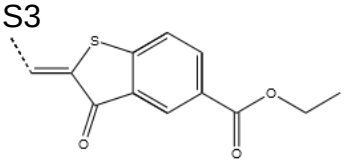	n.d.

Table 1 - Tested compounds. The left column states the name of the compound. The middle column shows the 2D-structure of the compound. The right column gives the IC50 values that were measured in *in vitro* experiments of Holy et al. with the compounds in hSERT (Dreier and Mihovilovic, Holy and Sitte, 2016). The concentrations are micromolar, the dates of the measurements are stated below each figure.

3.1 Conformational Search in MOE

Molecular Operating Environment (MOE) (Chemical Computing Group, 2017) is a computer based tool for molecular modelling and chemical computations. For getting familiar with the crystallized serotonin transporter protein, its binding sites and the protein-ligand interactions with the two co-crystallized escitalopram molecules of 5I73.pdb, the graphical interface of MOE was used.
The new molecules, azo-compounds and HTI-compounds, were created with the building panel provided by MOE.

The backbone of hSERT normally has no great movements especially when integrated in a membrane. On the contrary, the amino acid side chains are able to rotate freely, based on their environment and depending on the side chain. A ligand is also able to undergo several conformational changes when entering and binding to a protein. These movements allow a ligand to find a precise binding pocket in the protein.
The conformational search application is programmed to find the most probable conformation of a single molecule or a protein-ligand complex. The tool was used to calculate possible conformations of the photoswitchable compounds in the central binding site of hSERT.
Before starting the conformational search, an in-house script was run (7.1.1 Stochastic Pocket Script), which purpose was to select the ligand and seven residues, which stayed flexible during the computations. The following amino acids were chosen, because they lie closest to the ligand and define the central binding site: Arg104, Phe335, Glu493, Glu494, Val501, Thr497 and Tyr175. Glycines were left out as they have no relevant side chains. The rest of the protein was set to stay rigid, otherwise the calculations would affect all amino acids. This would take an unnecessary high amount of time, whereas only the interactions between the nearest binding site residues and the ligands were regard. In addition, more accurate results were anticipated by reducing the area of flexible bonds, because the conformational search function in MOE is provided for small to modest sized molecules.

There are a few options for the method, how the coordinates of the atoms will get perturbed such as LowModeMD, molecular dynamics, stochastic or systematic search. For the complex to be examined the stochastic search was chosen, where all bonds

rotate randomly. The idea behind was to get a greater variation of conformations than resulting from a systematic search, where the algorithm starts with the same bond rotation every time. The resulting pose would be closer to the most probable conformation. All other settings were left default: rejection limit 100, iteration limit 10.000, RMSD limit 0.25, energy window 7 kcal (Fig. 11).

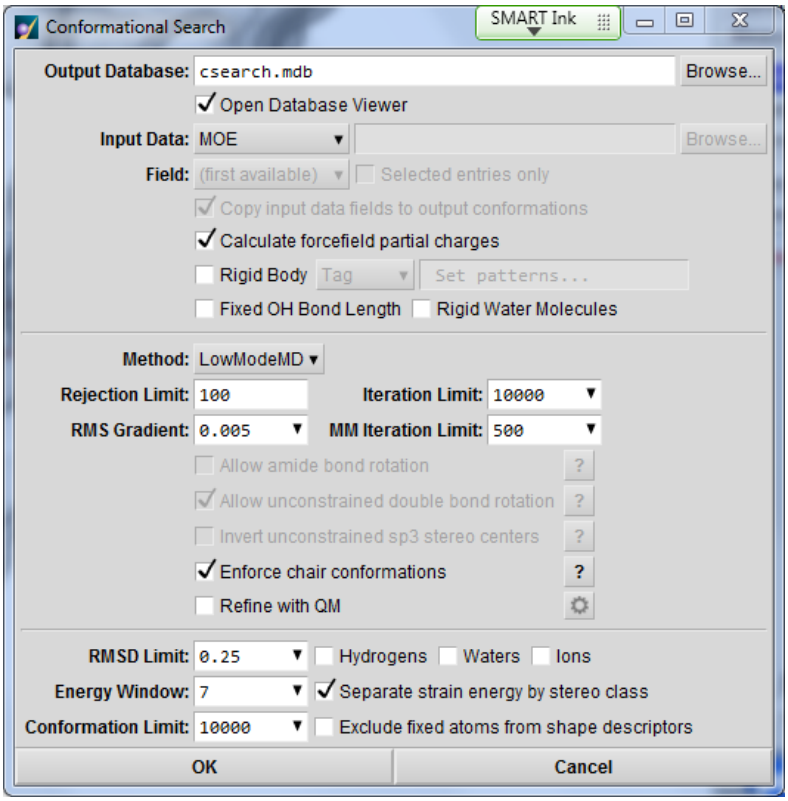

Fig. 11 - Conformational Search Panel in MOE

After calculating possible conformations, the algorithm minimizes the atoms of the resulting poses and saves it if it is different from the other results (calculated by RMSD values) and has reasonable strain energy.

The MOE user manual claims stochastic search not to be the first method of choice to calculate conformations because the algorithm spends a lot of time on minimizing conformations which do not have good enough values anyway to get into the pool of reasonable results. Therefore, it was decided to confirm the results via conformational search in another software, namely Schrödinger (Schrödinger, 2017).

3.2 Preparations for Schrödinger Software

Schrödinger is a software for drug discovery, molecular modelling and drug design providing a variety of applications to explore molecules, proteins or even complex structures of proteins and ligands. The graphical interface is called Maestro (Maestro | Schrödinger, 2017). It provides, inter alia, a building panel similar to the MOE building panel.

First, 5I73.pdb was imported into the Maestro workspace. The allosteric escitalopram molecule was removed. Escitalopram in the central binding site was modified by inserting a photoswitchable fragment instead of the original cyano-group. When selecting the whole new ligand, it was not recognized as one molecule by the software. Thus, the final compounds had to be built into hSERT in MOE and imported into Maestro for further calculations.

3.2.1 Protein Preparation Wizard

The Protein Preparation Wizard (Protein Preparation Wizard | Schrödinger 2017) adjusts the receptor protein by adding missing hydrogen atoms and correcting orientations of groups by minimizing the complex. The application prepares the protein for calculations in Schrödinger software.

3.3 Protein-Ligand Complex Refinement

The refinement tool (Prime | Schrödinger, 2017) finds the most probable pose and conformation of the ligand within the protein by prediction of rotamers of the side chains and subsequent minimization. The result is the most stable structure with the lowest calculated energy. Amino acids of the protein can be selected, which should be part of the refinement. The same residues of the central binding site as beforehand were chosen.

First, the hierarchical optimization was performed, which implemented the PGL sampling approach (Borrelli et al., 2010). PGL considered protein sidechains (P), ligand functional groups (G) and ligand orientational degrees of freedom (L). Rotamer

libraries were generated for all possible orientations of ligand functional groups by using a systematic sampling (1.0 Å and 30°). The rotamers were evaluated by a flexible steric-only scoring, then clustered and ranked by Prime Energy. The conformations with the lowest energy were delivered.
After the process ended, a local optimization within 5Å around the ligand was performed. The seed was set to “random” to increase the variety of resulting poses. If there were no great differences between the resulting poses of various runs with the same ligand, it can be assumed that the most probable pose has been predicted.

3.4 Prime MM-GBSA Energy Calculations

The Prime MM-GBSA application (= Molecular Mechanics Generalized Born Surface Area) (Prime | Schrödinger, 2017) calculates the binding energy between the ligand and the receptor protein. It does not give the absolute energy, but can be perfectly used as a scoring function and is therefore suitable to compare the binding energies of similar molecules. The difference between the free ligand and receptor, the complex is calculated (Equation 1). The binding energy, ΔG (bind), is negative, when the binding process is exotherm. In an exotherm reaction, the released energy is declared as negative value. Therefore, the lower the MM-GBSA energy value, the stronger is the binding and the more stable is the complex.

$$\Delta G\ (bind) = \Delta G\ (complex) - [\Delta G\ (free\ receptor) - \Delta G\ (free\ ligand)]$$

Equation 1 – Prime MM-GBSA calculates the binding energy of ligand and receptor by building the difference between the previously computed energy of the complex and the free, unbound receptor and ligand.

For investigation whether Z- or E-configuration of a ligand fit better into hSERT, the energy values had to deviate from each other. Only the ligands with the greatest differences between E- and Z- configuration were considered to be relevant for further investigations.
All settings were left default (Fig. 12).

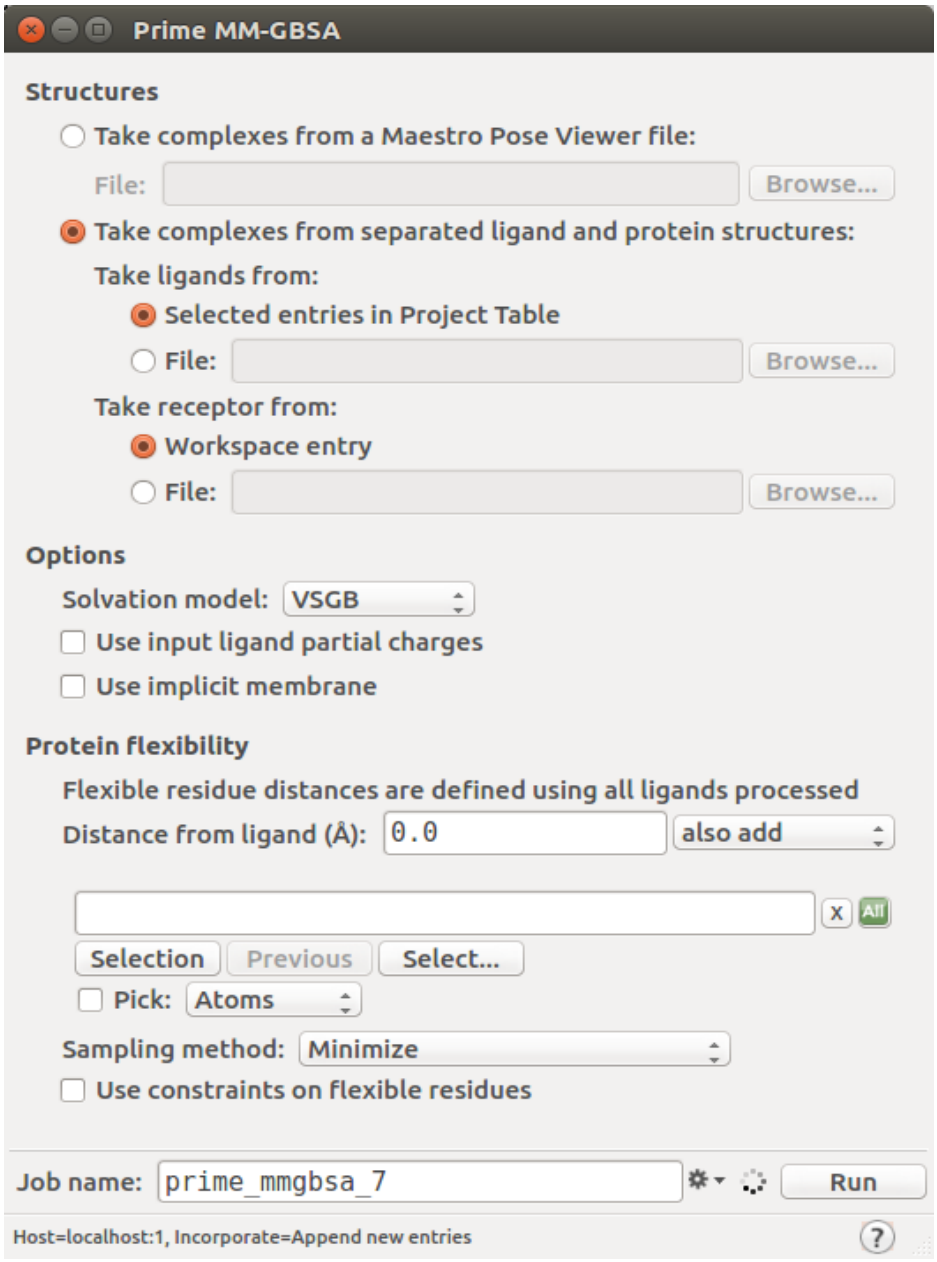

Fig. 12 – Prime MM-GBSA Panel in Schrödinger

3.5 Molecular Docking

Molecular Docking is a chemoinformatic method for prediction of the binding mode and binding energy of two molecules which are building a complex. It is a common method in pharmacoinformatics based research.
Several docking methods are possible, for example Schrödinger Glide Docking (Glide | Schrödinger, 2017), Schrödinger Induced Fit Docking (Induced Fit | Schrödinger, 2017), flexible docking with GOLD (Genetic Optimisation for Ligand Docking) (Jones et al., 1997).
Schrödinger Glide docking sets receptor and ligand rigid while finding a reasonable binding pose. Phe335 is able to switch to give place to the ligand as described above (Gabrielsen et al., 2012), therefore rigid docking does not seem appropriate for the present tests.
Schrödinger Induced Fit docking allows the complete protein and ligand to be flexible. As hSERT lies in a membrane, it is not freely flexible. Because of these results, the decision to work with GOLD (Jones et al., 1997) was made.

3.5.1 GOLD Docking

GOLD is a software for predictions of the correct binding mode, provided by The Cambridge Crystallographic Data Centre (CCDC). GOLD offers various settings within the docking protocol, which allows to include all the knowledge about hSERT into the docking algorithm, for instance flexibility, defining the binding site (Fig. 13), choosing out of four different scoring functions or setting constraints. The ligand and the protein have to be in a correctly protonated state. By defining the binding site, the residues were specified, which are adduced for the docking process.

```
<Gold.Protein.ActiveResidues>

TYR95 ASP98 TYR176 PHE335 THR497 VAL501 ILE172 PHE341 LEU443
THR439 ALA96 ALA169 ALA173 TYR175 SER336 GLY338 SER438 GLY442
GLY498 GLU493 ARG104
```

Fig. 13 - To work in GOLD, 21 binding site residues have to be selected.

3.5.1.1 Side Chain Flexibility

Residues of the binding site may be held flexible during docking. This tolerates torsional rotation within the amino acid side chains. The rotamer library (Lovell et al., 2000) provided by GOLD was used to define the possible torsion angles.

The more residues are kept flexible, the more conformational possibilities and space to explore arise during the docking process. Therefore, only amino acids should be selected, which are probable to move while ligand binding (Fig. 14).

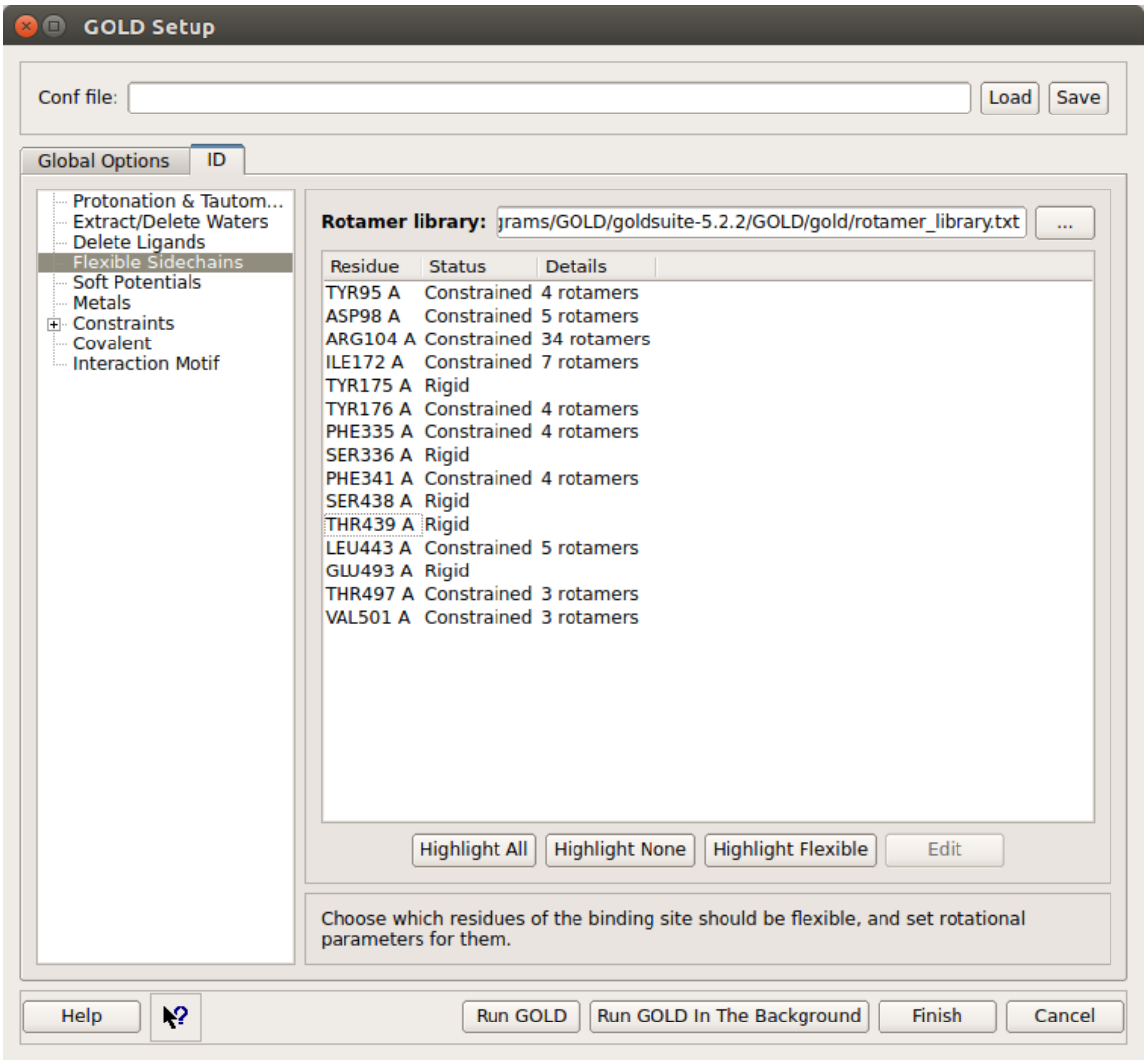

Fig. 14 – Side Chain Flexibility-panel in GOLD: Tyr95, Asp98, Arg104, Ile172, Tyr176, Phe335, Phe341, Leu443, Thr497, Val501 are able to move freely during the docking process.

3.5.1.2 Ligand Preparation

For defining the ligands, a database in MOE, containing the four structures, was created with E- and Z-configurations showing the greatest differences in the MM-GBSA energy calculation results (DD-355_E, DD-355_Z, DD-355_p_E, DD-355_p_Z, Table 1) and which are, for this reason, the most promising ligands. 100 GA (genetic algorithm) runs for each of the four ligands were chosen resulting in 400 poses.

3.5.1.3 Scoring Functions

There are four fitness functions (scoring functions) available in GOLD. Their different algorithms may lead to different rankings for the resulting poses. For generating poses, CHEMPLP was selected, which was set by default.

3.5.1.3.1 CHEMPLP

CHEMPLP (Piecewise Linear Potential) is the default scoring function in GOLD, because it is stated to be the most reliable function concerning pose prediction. The other scoring functions may be as accurate as CHEMPLP in predicting a binding pose in certain protein complexes. CHEMPLP works as an empirical fitness function and is optimized to calculate the steric compatibility of protein and ligand. Heavy-atom clashes, torsional potentials as well as flexible side chains are considered for docking calculations.

3.5.1.3.2 GoldScore

The algorithm of GoldScore considers the protein-ligand hydrogen bond energy, the protein-ligand van der Waals energy, the ligand internal van der Waals energy and the ligand torsional strain energy. This fitness function has been designed to predict the ligand binding pose, rather than to calculate binding affinities.

3.5.1.3.3 ChemScore

ChemScore fitness function was derived from binding affinity values of a set of protein-ligand complexes. This algorithm calculates the total free energy which is released during docking of ligand and receptor, considering clashes and torsional energy to prevent poor conformations.

3.5.1.3.4 ASP

The ASP (Astex Statistical Potential) fitness function's accuracy can be compared to GoldScore and ChemScore. It uses a protein database to find information about frequent atom-atom interactions of existing protein-ligand complexes to create statistical potentials. The results depend on the database the scoring function gets its information from. A general scoring function, like provided in GOLD, uses the entire database, while specifying a protein family for calculations could lead to more precise results.

3.6 Rescoring

Each fitness function scores the generated docking poses by different criteria. GOLD provides a rescoring function for a better interpretation of the results. The docking run output poses were rescored with each scoring function available (ChemPLP, GoldScore, ChemScore, ASP) to find the best function for the respective protein-ligand complex.

3.7 Common Scaffold Clustering

Common Scaffold Clustering is a method which divides all poses resulting from a docking run into clusters considering the RMSD (see 3.8) of the heavy atoms of their common scaffold. The assumption is that highly active compounds with a common scaffold show the same binding mode in the protein binding pocket whereas compounds with low activity cannot adopt this conformation. The method can therefore be used to find a common binding mode which shows the important interactions between protein and ligand and the most probable binding pose of the ligand.
In the present case, the escitalopram scaffold was used without the cyano group (Fig. 15, Fig. 16) as common scaffold of the 400 docking poses. The distance threshold was set at 3Å.

```
Fc1ccc(C2(CCC[N+](C)C)OCc3c2cccc3)cc1
```

Fig. 15 - SMILES string of the common scaffold

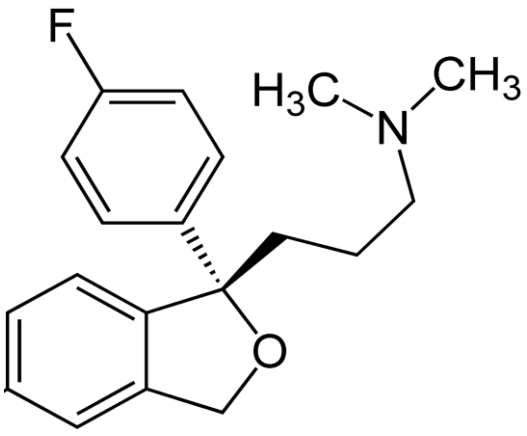

Fig. 16 - common scaffold

For running the in-house script for common scaffold clustering RStudio (RStudio Team, 2015) was used.

3.8 RMSD-Matrix

The RMSD (root-mean-square deviation) (Equation 2) is used to measure the differences between given values for example the distance between heavy atoms (C, N, O) and therefore the similarity between protein or bound ligand structures.

$$RMSD = \sqrt{\frac{1}{N}\sum_{i=1}^{N}\delta_i^2}$$

Equation 2 – RMSD equals the root of the mean differences between the atoms squared, where δi is the distance between atom i and either a reference structure or the mean position of the N equivalent atoms.

3.9 Correlation Plots

To illustrate the resulting poses, the energy values calculated by the different scoring functions were plotted against each other to see how they correlate.

4 Results and Discussion

4.1 Building Ligands in MOE

First, the azo- and HTI-structures of Table 1 were built in MOE. The escitalopram molecule in the central binding site of hSERT in 5I73_CS.pdb was replaced by the compound to be tested. The visual examination of the ligands in the unchanged binding site led to detection of additional clashes of the attached parts of the molecule with binding site residues. Especially conspicuous was the fact that the attached part of every tested ligand showed clashes with one of the residues, Phe335.

The 2D ligand interactions panels (Fig. 17) support the indication that the Z-configurations fit better into the binding site than the E-configurations because the substituent to the azo-group does not fit into the pocket.

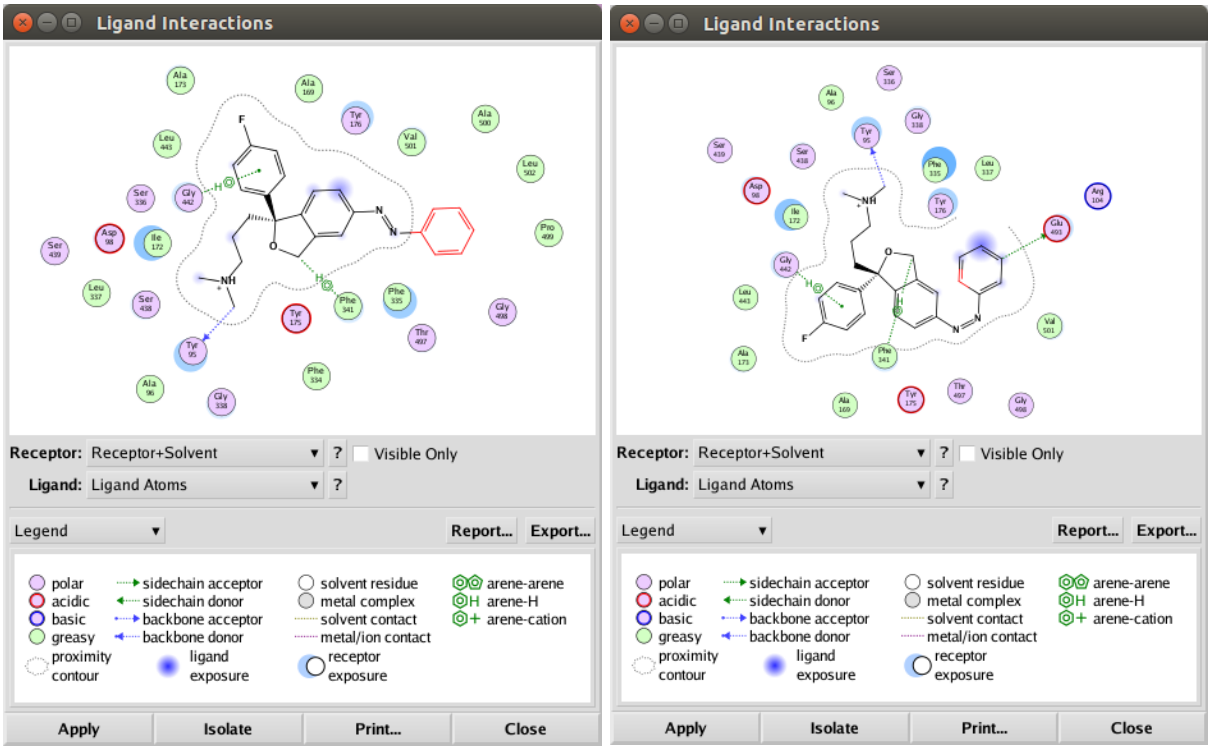

Fig. 17 – 2D ligand interactions panels in MOE. Left: DD-321 in E-configuration. The red colour of the phenyl ring indicates that it clashes with many residues of the protein binding site and does not fit into it. Right: DD-321 in Z-configuration.

When attaching different substituents in para-position to the phenyl rest, like *p*-Br, *p*-Me, *p*-Cl, *p*-OH, *p*-COOH and *p*-COOMe, there were not more clashes in comparison to DD-321, the unsubstituted phenyl ring. However, an attachment in *meta*-position, *m*-CN, showed additional clashes. From these findings was concluded that for the given azo-compounds the combination of Z-configuration and *para*-positioned substituent seemed optimal.

The visual examination of the new built ligands in hSERT was expected to only give an overview of the compounds possibly fitting into the central binding site. Potential conformational changes within the binding site residues were not yet taken into consideration during this early phase of the research project.

For further investigations and to find out which residues may interact with the compounds of interest was required.

4.2 Conformational Search in MOE

Via conformational search small conformational rotation changes of the amino acids which were nearest to the ligand and of the substituents attached to the escitalopram-scaffold were considered.

After the first conformational search runs it became obvious, that Phe335 is able to change its conformation to give way to the ligand. This phenomenon was confirmed by examining literature (1.3.2 Extracellular Gate). Further investigations by conformational searches showed that Phe335 always switched to give place for the compounds in E-configuration. The ligand then reached into the allosteric binding site.

4.2.1 Azo-Compounds

The tested azo-compounds had no very big steric differences and all of them fit into the binding site when Phe335 switched and cleared the way into the allosteric binding site. It was noticed, that in contrary to Z-configurations, for E-configurations Phe335 always had to switch that the ligand fits into the binding pocket.

Thereafter, the angles and dihedral angles of the resulting ligand conformations were examined and compared to knowledge from literature. A simple diphenylazo compound was built in MOE (Fig. 18, Fig. 19) (SMILES code of the trans-azo-compound: N(=N/c1ccccc1)\c1ccccc1, SMILES code of the cis-azo-compound: N(=N\c1ccccc1)\c1ccccc1), minimized and its angles and dihedral angles were measured. The trans-azo-compound was planar, which indicated that it was more stable than the cis-compound.

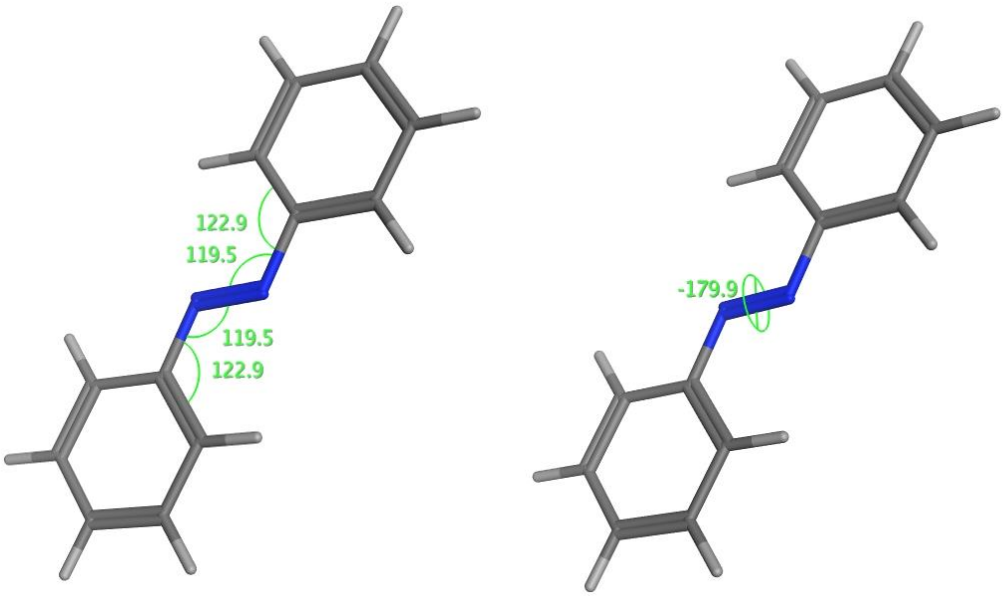

Fig. 18 – Trans-conformation of the diphenylazo compound in MOE. Left: Values of angles between the diazo bond and the phenyl rings. Right: Values of the dihedral angle between the diazo bond and the phenyl rings.

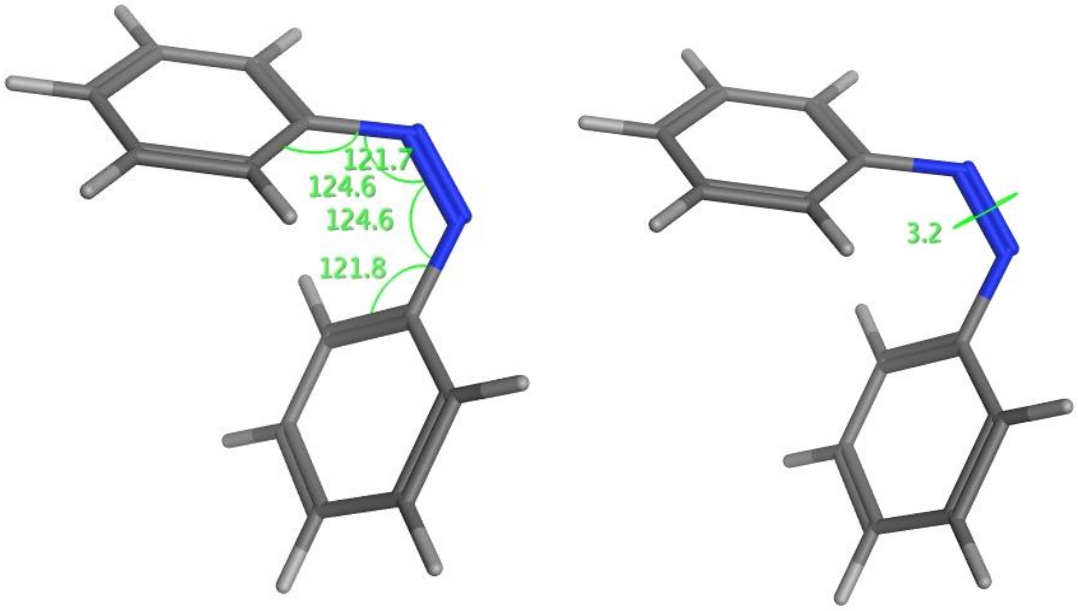

Fig. 19 – Cis-conformation of the diphenylazo compound in MOE. Left: Values of angles between the diazo bond and the phenyl rings. Right: Values of the dihedral angle between the diazo bond and the phenyl rings.

4.2.2 HTI-Compounds

Because of the results of the tested azo-compounds, the HTI-compound with the bulkiest side chain was chosen for a start (DD-355). The probability seemed higher that the ligand fits into the binding site only in one of its configurations while the other one leads to improbable steric conformations or dihedral angles and clashes with the binding pocket residues.

By examining the resulting poses, DD-355 in Z-configuration was found to show greater steric deviations than its E-counterpart and twisted dihedral angles (Fig. 20). Furthermore, DD-355_E reaches towards the escitalopram molecule in the allosteric binding site, which the pose in Z-configuration does not. This suggests that DD-355 is more likely to fit into hSERT in E-configuration than in Z-configuration.

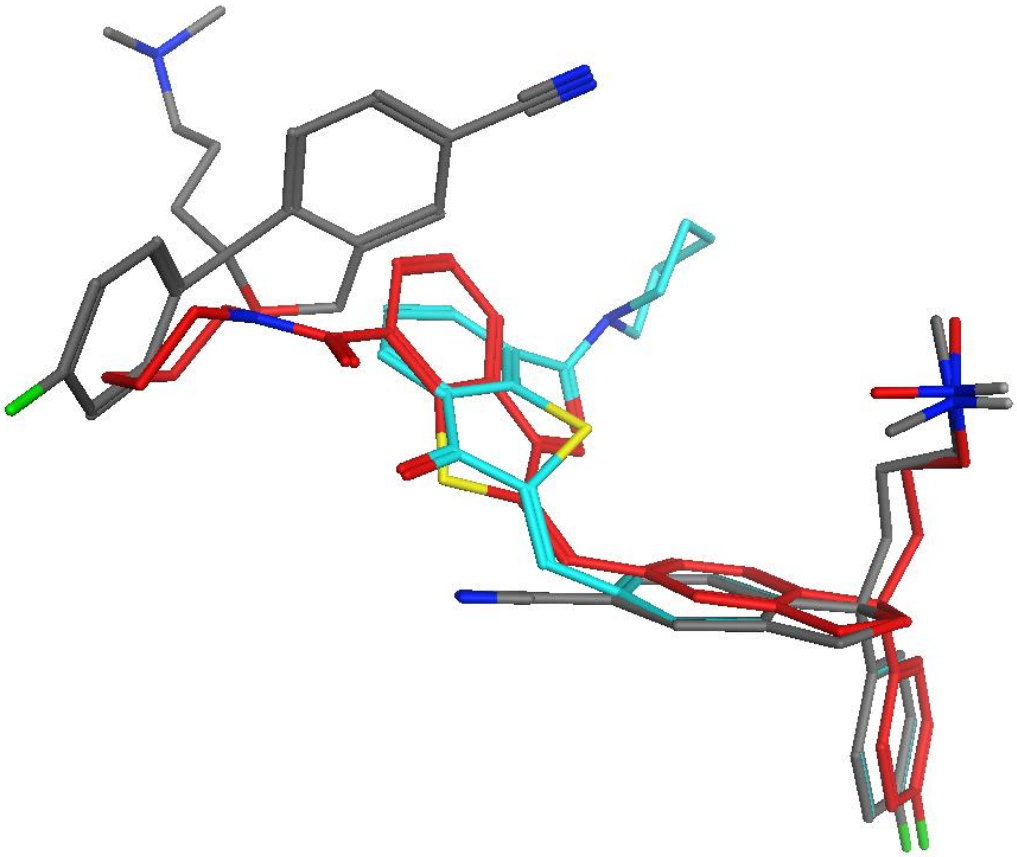

Fig. 20 - Resulting poses of two conformational search runs in MOE. Grey: Escitalopram in central (below) and allosteric binding site (above). Red: DD-355_E, reaches into the allosteric binding site. Cyan: DD-355_Z.

4.2.3 Conclusion of the Conformational Search in MOE

Summing up the conformational search results led to the assumption, that all of the tested azo-ligands fit into the central binding pocket of hSERT regardless their configuration, because Phe335 switches to enable the ligand to reach into the allosteric binding site. These results support the biological data (Table 1).

After comparing the resulting poses of several conformational search runs, it appeared that repeated calculations with the same ligand led to different results, when the conformation of the starting position was manually changed slightly to reduce the clashes (Fig. 21). Noticing that the claimed best conformation depends on the starting position of the ligand implies that the conformational search tool only can be used for vague assumptions of how the ligand might adjust itself into the transporter. More

significant results can be reached when calculating the binding energy between the ligand and hSERT and compare the resulting energy values of the two configurations.

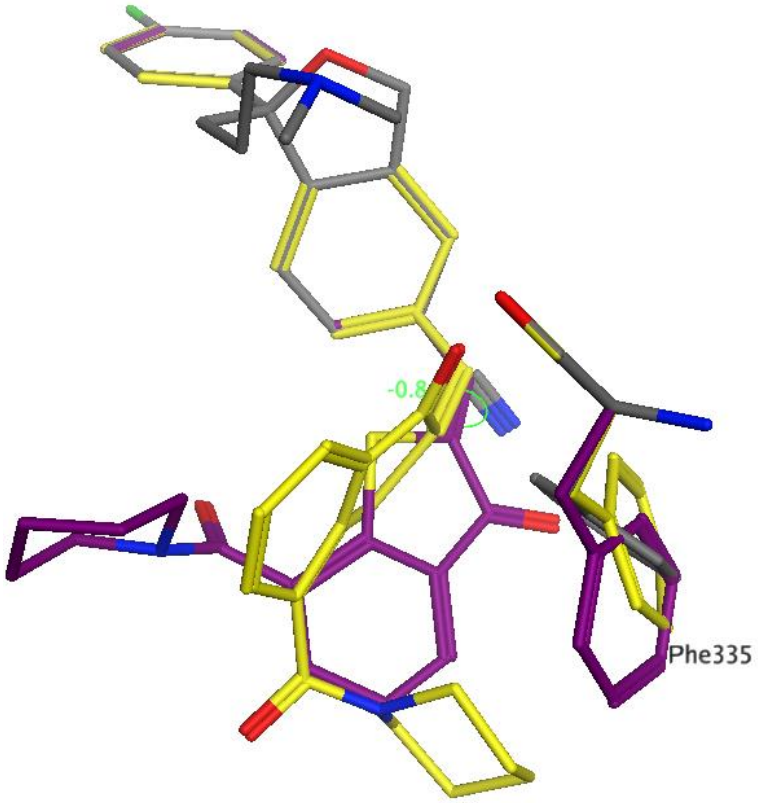

Fig. 21 – Resulting poses of two conformational search runs of the same ligand, DD-355_Z in MOE. Grey: Escitalopram in the central binding site. Yellow: Output of run 1, starting pose with clashes, dihedral angle of HTI part 60.0°, HTI-part directed in allosteric binding site. Violet: Output of run 2, starting position with rotated **Ar-C**=C-R so that ligand shows less clashes, dihedral angle -0.8°. In this case Phe335 did not switch, but the HTI-substitutes point into different directions.

4.3 Binding Energy Calculation

The work with Schrödinger software raised a new problem. When the escitalopram molecule of 5I73_CS.pdb was replaced with the first ligand, DD-355, by building it with the fragments provided by Maestro, the ligand was not recognized as one entire molecule. When working with the protein-ligand complex refinement tool, the whole ligand needed to be selected for calculating a possible pose. Therefore, the structure was built into hSERT in MOE and imported into Schrödinger software. This strategy worked, the ligand was recognized as one entire molecule by the refinement tool.
The output of the protein-ligand complex refinement provided the most probable pose the ligand would occupy in the transporter protein. Subsequently, the binding energy between the ligand and the protein was calculated. The lower the resulting energy, the more stable is the complex. Every structure was recalculated several times, always starting with importing the complex anew, to reduce possible bias of the program. Altogether the binding energy values for ten HTIs and nine azo-compounds were calculated.

4.3.1 Azo-Compounds

The resulting energy values (7.1.2 Results of the Binding Energy Calculations in detail) comparing E- and Z-configuration showed an orientation towards ligands in E-configuration. Most of the tested compounds in E-configuration have lower energy values than their Z-counterpart. However, compared to the differences in the outcoming HTI values, the azo-compound results seem not to be significant (acquired variance ≤0.05). The slightly lower energy values belonging to most of the tested ligands in E-configuration may correlate with the planar structure of E- or trans-azo-compounds. These are more stable and have therefore a lower basic energy than Z- or cis-compounds, which show higher strain within their angles. This fact could explain the phenomenon that some tested Z-compounds switched their configuration into E-configuration while calculation of the best pose by the refinement tool. Unfortunately, the protein-ligand refinement tool provides no option to secure the configuration during the computation process.

One outlier was found, where the resulting energy values were lower in Z-configuration, DD-261. More interactions between ligand in E-configuration and protein binding site residues such as hydrogen bonds or π-π-interactions were discovered, which leaves no possible explanation, because the interactions indicate to the opposite outcome.
To sum up, several reasons confirm the assumption that was made after the conformational search in MOE: The steric deviations within the azo-compounds are not big enough to result in significant differences comparing E- and Z-configuration.

4.3.2 HTI-Compounds

Further investigations of HTI-compounds showed that DD-355 confirmed the assumption of significant differences in binding energy values between E- and Z-configuration. The E-configuration of DD-355 binds with a mean energy value of -119.57 kcal/mol, whereas the Z-configuration reaches only -108.09 kcal/mol (difference=11.48) (Fig. 22).
The greatest difference of energy values was calculated between E- and Z-configuration of DD-355_p, an on-paper-designed new ligand, where the piperidinyl-ring is substituted in *para*-position to the sulphur in the thioindigo-ring, whereas in DD-355 it is located in *meta*-position. Surprisingly and in contrast to DD-355 the Z-configuration of DD-355_p showed the higher affinity to hSERT with an energy value of -130.46 kcal/mol, whereas the E-configurational ligand was measured with -107.87 kcal/mol (difference=22.59). The variance and standard deviation of the four test runs each support these figures by significant values ($v \leq 0.05$) with v=0.02, s=0.15 for E-configuration but v=0.13, s=0.36 for Z-configuration (Fig. 23).

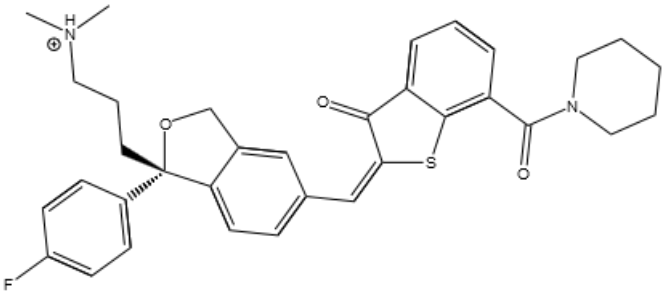

E-conf.	Z-conf.
x=**-119.47**	x=-108.09
v=0.4068	v=5.4634
s=0.6378	s=2.3374

Fig. 22 - Left: structure of DD-355, right: mean value, variance and standard deviation of MM-GBSA calculation results of E- and Z-configuration. The lower energy is highlighted in bold letters.

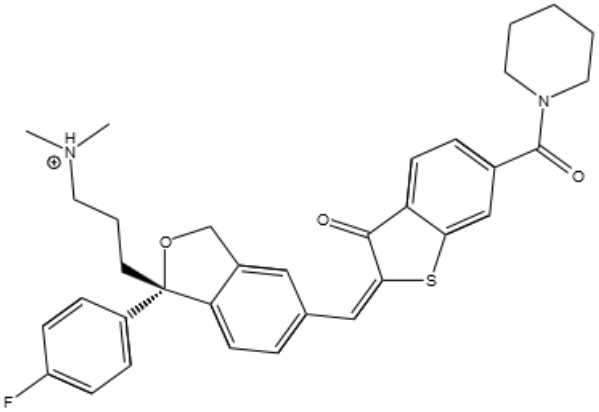

E-conf.	Z-conf.
x=-107.87	x=**-130.46**
v=0.0226	v=0.1297
s=0.1504	s=0.3601

Fig. 23 - Left: structure of DD-355_p, right: mean value, variance and standard deviation of MM-GBSA calculation results of E- and Z-configuration. The lower energy is highlighted in bold letters.

Neither of the other tested compounds showed that great and significant differences in their binding energy (extended data). There is no trend visible, if overall E- or Z-configuration is favoured. The assumption to observe conspicuous lower figures when the ligand showed interactions like hydrogen bonds or even less clashes with the transporter protein, was rebutted by the absence of such findings in the resulting poses.

Regarding the biological experimental data, DD-350, the HTI-compound substituted with an acid (R-COOH) is about ten times more active than the methyl- and the ethylester (DD-353 and DD-354). Arg104 and Glu494 occurred to build a hydrogen bridge in the current outward-open state. The acid group of the tested ligand seemed

to reach towards these residues close enough to possibly interact with one of them when adopting its deprotonated form ($R\text{-}COO^-$). Upon this possibility and the fact that it is unknown whether the acid exists protonated or deprotonated in the binding site of hSERT, both conditions were tested. Two of the four test runs with the deprotonated Z-configuration of DD-350 ($DD\text{-}350^-$) resulted in slightly lower energy levels than the other outcomes of DD-350. These two poses interacted with Arg104. However, the values did not distinguish much, for that reason we left them out of account. Furthermore, neither of the results for the ligands substituted with the acid, the methyl- or the ethyl-group confirmed the distinct difference given by the biological data (Table 1).

4.3.3 Conclusion of the Binding Energy Calculation

The MM-GBSA calculations gave a good insight to the binding properties of the tested ligands in hSERT. Advantages of the method were found, but its limits were discovered. An auspicious point was observed in correlation between lower binding energy and the resulting pose's proximity to escitalopram in the crystal structure. In most cases of tested HTI-compounds the resulting pose reaching into the allosteric binding site showed the lower energy, which indicates that instead of clashing with central binding site residues these poses found enough place in hSERT and therefore settled more stably. Possible limitations of the method appear in testing the azo-compounds, which have less distinction in their steric structure. All tested E-configurations of azo-compounds show slightly better MM-GBSA energy values than their Z-equivalent. A possible reason is that Z-configurations have higher strain within their angles. Furthermore, like the output molecules of MOE conformational search, the MM-GBSA values too depend on the starting positions of the ligands in several cases, especially azo-compounds.

4.4 Docking and Common Scaffold Clustering

The method of choice for validation of the MM-GBSA calculation results was docking. Therefore, the focus was laid on DD-355 and DD-355_p, because they had the most promising results. The docking program was fed with the four different ligands, Z- and E-configuration of each of the two compounds. 100 poses of each ligand were calculated and a database containing the 400 resulting poses was generated. Thereafter, a common scaffold was defined, a RMSD matrix of the resulting poses was calculated and the poses were clustered in RStudio.
For evaluation of the resulting poses, several procedures were applied. Selection of the clusters, which contain the most poses, led to the best scored poses. Scoring the poses by different algorithms showed if there are poses favoured by all fitness functions. Therefore, the ten best scored poses of every scoring function and the best scored poses within the best cluster were computed. Examination of the proximity of the docking results to the crystal structure provided an indication for the activity. The closer to the original escitalopram molecule bound to hSERT, the resulting pose was classified to be more probable. Inspection whether the resulting pose reached into the allosteric binding site gave indication of the probability of the pose. Orientation into the allosteric binding site meant less clashes and therefore higher stability.

4.4.1 Clusters

The output of the docking run and common scaffold clustering divided the 400 poses into 19 clusters at a distance threshold of 3Å (Fig. 24). The best scored compounds were expected in cluster 1, but this should also have been the cluster containing the most poses. In this case, cluster 2 holding 112 of them was the largest. For better overview, all clusters containing less than 20 poses were removed, remaining clusters 1, 2, 4, 5, 6, 7, 8, 13, 14. Cluster 1 stayed as well for being interesting whether itself or cluster 2 held the best scored poses.

1	2	3	4	5	6	7	8	9	10
9	112	2	36	36	58	21	28	2	4
11	**12**	**13**	**14**	**15**	**16**	**17**	**18**	**19**	
2	5	21	26	1	4	18	6	9	

Fig. 24 – first and third row: number of cluster, second and fourth row: number of contained poses.

The graph in Fig. 25 demonstrates the distribution of docking poses within the clusters. Cluster 2 distinctly is the largest cluster. It contains poses of each of the four ligands in rather the same amount of poses per ligand.

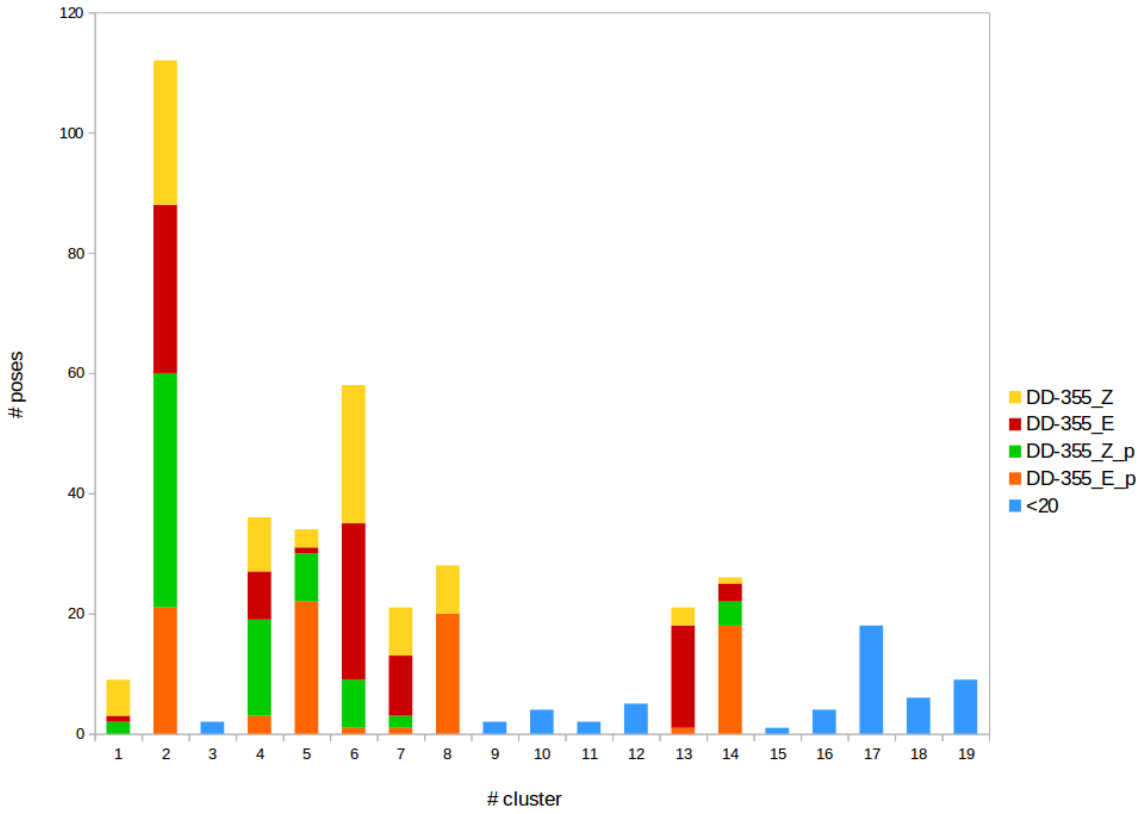

Fig. 25 - The graph shows the distribution of docking poses within the clusters. On the x-axis the clusters are listed by their number. The y-axis gives the number of poses in each cluster. The colors describe the ligands. Clusters containing less than 20 poses were not divided into the contained compounds (except cluster 1).

The correlation plot (Fig. 26) showed the correlation between the docking poses ranked with two different scoring functions. The higher the poses were scored, the better they fit into the central binding site. The majority of poses in cluster 2 was concentrated in the right upper corner of the plots (circled entries), which confirmed the assumption, that cluster 2 contained the best scored poses within every scoring function. Concluding of the RMSD values, all values were below 1.5, which proved that the poses resembled the crystal structure.

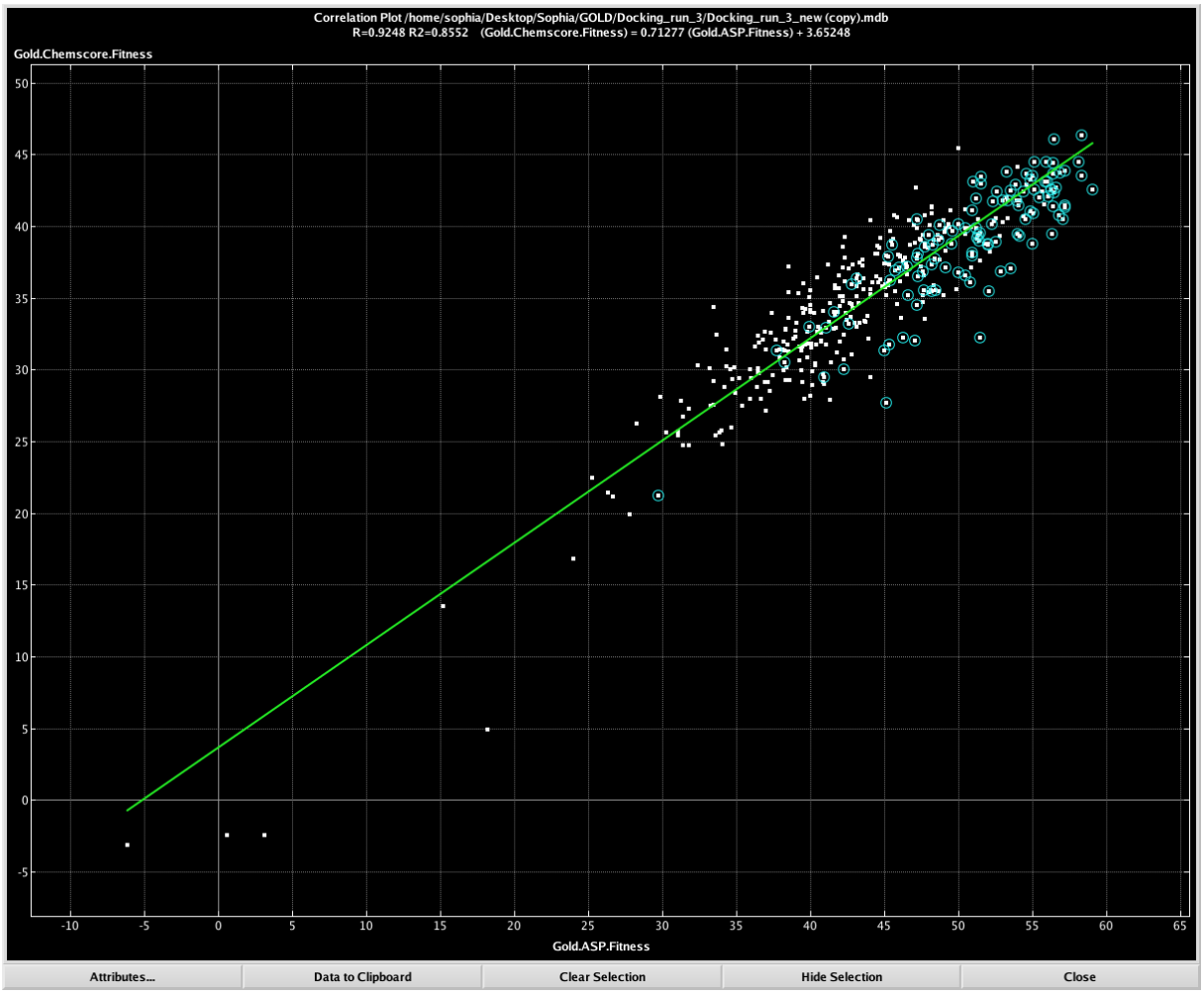

Fig. 26 - Correlation plot of ChemScore and ASP. R2=0.86, circled entries belong to cluster 2.

4.4.2 Rescoring

9 out of the 10 poses the default scoring function ChemPLP ranked as the best were part of cluster 2. Rescored by ASP 8 out of the 10 best scored were contained in cluster 2, with GoldScore it were 7 out of 10 and with ChemScore 8 out of 10 best scored poses belonged to cluster 2. The four fitness functions confirmed each other in this content.
When ranking only the poses of cluster 2, ASP showed that 9 out of the 10 were poses of the Z-configuration of DD-355_p, one pose was an E-configuration of DD-355. ASP supported the outcome of MM-GBSA calculation, where the Z-configuration of DD-355_p like the E-configuration of DD-355 showed clearly higher activity than their counter-configurations.

4.4.3 Orientation of the Poses

Proximity to the crystal structure is an important indication for the reliability of the docking poses. The crystal structure of hSERT gave an example of how escitalopram and hSERT interact in a stable complex. Therefore, the assumption was made, that with the proximity to the crystal structure the docking poses gain stability and prapability which results in favourable poses.
All poses of cluster 2 and cluster 4 lied superposable to escitalopram in the crystal structure. Neither in cluster 1 nor in one of the other examined clusters all poses fit the crystal structure. In both mentioned clusters the substituted HTI-parts of the ligands reached into the allosteric binding site. Comparing these results to the outcomes of MM-GBSA calculations, it was noticeable that the compounds predicted as best fitting into the central binding site of hSERT, E-configuration of DD-355 and Z-configuration of DD-355_p, both reached into the allosteric binding site whereas their counterparts, Z-configuration of DD-355 and E-configuration of DD-355_p, did not point towards the allosteric binding site.

5 Conclusion and Outlook

Various binding energy predicting tests were performed in this diploma thesis. They conclude in the assumption that at least two escitalopram-scaffold HTI-compounds exist, which show markedly higher affinities to the central binding site of hSERT in one of their configurations than in the counter-configuration. In case of DD-355, the more active compound adopts E-configuration, whereas with DD-355_p, the Z-configuration shows the higher affinity than the E-configuration. The performed docking studies support the affinities of these compounds to the central binding site of hSERT. Testing the predicted compounds in biological systems would provide further information concerning the binding affinities to the central binding site of hSERT and the possibility to include photoswitchable drugs for analysis as well as in human medical treatment. A drug molecule provided with a photoswitchable fragment could be inserted to the body in its inactive configuration and could then selectively be activated at the target location by stimulation with light and thereby change to the active configuration. The selective activation of the drug at the target site results in less side effects because in the rest of the body the substance stays inactive. Furthermore, when the light source is extinguished, the photoswitchable structure automatically switches back into its inactive configuration and therefore, the duration of the drugs effect can be controlled (Mehta et al., 2017). Investigation of photoswitchable drugs targeting the human serotonin transporter enables new possibilities for development of new antidepressant drugs with less side effects.

6 Bibliography

Benkert, Otto, and Hanns Hippius. 2016. *Kompendium der Psychiatrischen Pharmakotherapie*. 11th ed. Springer-Verlag.

Berman, Helen M., John Westbrook, Zukang Feng, Gary Gilliland, T. N. Bhat, Helge Weissig, Ilya N. Shindyalov, and Philip E. Bourne. 2000. 'The Protein Data Bank'. *Nucleic Acids Research* 28 (1):235–42.

Borrelli, Kenneth W., Benjamin Cossins, and Victor Guallar. 2010. 'Exploring Hierarchical Refinement Techniques for Induced Fit Docking with Protein and Ligand Flexibility'. *Journal of Computational Chemistry* 31 (6):1224–35. https://doi.org/10.1002/jcc.21409.

Boyer, Edward W. 2016. 'Serotonin Syndrome (Serotonin Toxicity)'. https://www.uptodate.com/contents/serotonin-syndrome-serotonin-toxicity.

Molecular Operating Environment (MOE), 2013.08; Chemical Computing Group ULC, 1010 Sherbooke St. West, Suite #910, Montreal, QC, Canada, H3A 2R7, 2017

Cipriani, Andrea, Marianna Purgato, Toshi A Furukawa, Carlotta Trespidi, Giuseppe Imperadore, Alessandra Signoretti, Rachel Churchill, Norio Watanabe, and Corrado Barbui. 2012. 'Citalopram versus Other Anti-Depressive Agents for Depression'. *The Cochrane Database of Systematic Reviews* 7 (July):CD006534. https://doi.org/10.1002/14651858.CD006534.pub2.

Coleman, Jonathan A., Evan M. Green, and Eric Gouaux. 2016. 'X-Ray Structures and Mechanism of the Human Serotonin Transporter'. *Nature* 532 (7599):334–39. https://doi.org/10.1038/nature17629.

Cross, L. C., and W. Klyne. 1974. 'Rules for the Nomenclature of Organic Chemistry: Section E: Stereochemistry (Recommendations 1974)', no. 45:11–30.

Dreier, Dominik, and Marko Mihovilovic. n.d. TU Vienna, Institute of Applied Synthetic Chemistry, Getreidemarkt 9, 1060 Wien.

Gabrielsen, Mari, Rafał Kurczab, Aina W. Ravna, Irina Kufareva, Ruben Abagyan, Zdzisław Chilmonczyk, Andrzej J. Bojarski, and Ingebrigt Sylte. 2012. 'Molecular Mechanism of Serotonin Transporter Inhibition Elucidated by a New Flexible Docking Protocol'. *European Journal of Medicinal Chemistry* 47 (1):24–37. https://doi.org/10.1016/j.ejmech.2011.09.056.

'Glide | Schrödinger'. n.d. Accessed 19 June 2017. https://www.schrodinger.com/glide.

Gómez-Santacana, Xavier, Silvia Pittolo, Xavier Rovira, Marc Lopez, Charleine Zussy, James A. R. Dalton, Adèle Faucherre, et al. 2017. 'Illuminating Phenylazopyridines To Photoswitch Metabotropic Glutamate Receptors: From the Flask to the Animals'. *ACS Central Science* 3 (1):81–91. https://doi.org/10.1021/acscentsci.6b00353.

Green, Evan M., Jonathan A. Coleman, and Eric Gouaux. 2015. 'Thermostabilization of the Human Serotonin Transporter in an Antidepressant-Bound Conformation'. *PLoS ONE* 10 (12). https://doi.org/10.1371/journal.pone.0145688.

Holy, Marion, and Harald Sitte. 2016. Institut für Pharmakologie, 1090 Wien: Medizinische Universität Wien.

'Induced Fit | Schrödinger'. n.d. Accessed 19 June 2017. https://www.schrodinger.com/induced-fit.

Irie, M. 2000. 'Photochromism: Memories and Switches Introduction'. *Chemical Reviews* 100 (5):1683–84. https://doi.org/10.1021/cr980068l.

Jones, Gareth, Peter Willett, Robert C Glen, Andrew R Leach, and Robin Taylor. 1997. 'Development and Validation of a Genetic Algorithm for Flexible

docking1'. *Journal of Molecular Biology* 267 (3):727–48. https://doi.org/10.1006/jmbi.1996.0897.

Katsonis, N, M Lubomska, M Pollard, B Feringa, and P Rudolf. 2007. 'Synthetic Light-Activated Molecular Switches and Motors on Surfaces'. *Progress in Surface Science* 82 (7–8):407–34. https://doi.org/10.1016/j.progsurf.2007.03.011.

Kristensen, Anders S., Ulf Simonsen, and Jacob Andersen. 2011. 'SLC6 Neurotransmitter Transporters: Structure, Function, and Regulation | Pharmacological Reviews'. 2011. http://pharmrev.aspetjournals.org/content/63/3/585.long.

Leach, Andrew R. 2001. 'Leach - Molecular Modelling. Principles and Applications (2001).pdf'. 2001. http://biomodeling.org.ua/Books/Leach%20-%20Molecular%20Modelling.%20Principles%20and%20Applications%20(2001).pdf.

LeVine, Michael V., Michel A. Cuendet, George Khelashvili, and Harel Weinstein. 2016. 'Allosteric Mechanisms of Molecular Machines at the Membrane: Transport by Sodium-Coupled Symporters'. *Chemical Reviews* 116 (11):6552–87. https://doi.org/10.1021/acs.chemrev.5b00627.

Lovell, S. C., J. M. Word, J. S. Richardson, and D. C. Richardson. 2000. 'The Penultimate Rotamer Library'. *Proteins* 40 (3):389–408.

Schrödinger Release 2015-2: Maestro, Schrödinger, LLC, New York, NY, 2017

Meer, Edmund te. 1876. 'Ueber Dinitroverbindungen Der Fettreihe'. In *Justus Liebig's Annalen Der Chemie*, 181:1–22.

Mehta, Zenobia B., Natalie R. Johnston, Marie-Sophie Nguyen-Tu, Johannes Broichhagen, Peter Schultz, Dean P. Larner, Isabelle Leclerc, Dirk Trauner, Guy A. Rutter, and David J. Hodson. 2017. 'Remote Control of Glucose Homeostasis in Vivo Using Photopharmacology'. *Scientific Reports* 7 (1):291. https://doi.org/10.1038/s41598-017-00397-0.

myHealthbox. n.d. 'FI Cipralex 10 Mg - Filmtabletten'. myHealthbox. Accessed 21 June 2017a. https://myhealthbox.eu.

———. n.d. 'FI Floxyfral 50 Mg - Filmtabletten'. myHealthbox. Accessed 21 June 2017b. https://myhealthbox.eu.

Penmatsa, Aravind, Kevin H. Wang, and Eric Gouaux. 2013. 'X-Ray Structure of Dopamine Transporter Elucidates Antidepressant Mechanism'. *Nature* 503 (7474):85–90. https://doi.org/10.1038/nature12533.

Plenge, Per, Lei Shi, Thijs Beuming, Jerez Te, Amy Hauck Newman, Harel Weinstein, Ulrik Gether, and Claus J. Loland. 2012. 'Steric Hindrance Mutagenesis in the Conserved Extracellular Vestibule Impedes Allosteric Binding of Antidepressants to the Serotonin Transporter'. *The Journal of Biological Chemistry* 287 (47):39316–26. https://doi.org/10.1074/jbc.M112.371765.

Schrödinger Release 2015-2: Prime, Schrödinger, LLC, New York, NY, 2017

Schrödinger Release 2015-2: Schrödinger Suite 2015-2 Protein Preparation Wizard; Epik, Schrödinger, LLC, New York, NY, 2016; Impact, Schrödinger, LLC, New York, NY, 2016; Prime, Schrödinger, LLC, New York, NY, 2017

Pruthi, Sandhya. n.d. 'Tricyclic Antidepressants (TCAs)'. Mayo Clinic. Accessed 21 June 2017. http://mayoclinic.org.

Ramamoorthy, Sammanda, Toni S. Shippenberg, and Lankupalle D. Jayanthi. 2011. 'Regulation of Monoamine Transporters: Role of Transporter Phosphorylation'. *Pharmacology & Therapeutics* 129 (2):220–38. https://doi.org/10.1016/j.pharmthera.2010.09.009.

Rot, Marije aan het, Sanjay J. Mathew, and Dennis S. Charney. 2009. ‘Neurobiological Mechanisms in Major Depressive Disorder’. *CMAJ : Canadian Medical Association Journal* 180 (3):305–13. https://doi.org/10.1503/cmaj.080697.

‘RStudio Team’. 2015. *RStudio* (blog). 2015. https://www.rstudio.com/.

Sauermost, Rolf. 1999. ‘Lexikon Der Biologie’. 1999. http://www.spektrum.de/lexikon/biologie/serotonin/61183.

‘Schrödinger’. n.d. Accessed 3 July 2017. https://www.schrodinger.com/.

Smyth, M S, and J H J Martin. 2000. ‘X Ray Crystallography’. *Molecular Pathology* 53 (1):8–14.

‘U.S. Food and Drug Administration’. 2017. 2017. https://www.accessdata.fda.gov/scripts/cder/daf/index.cfm?event=overview.process&ApplNo=011838.

Wiedbrauk, Sandra, and Henry Dube. 2015. ‘Hemithioindigo—an Emerging Photoswitch’. *Tetrahedron Letters* 56 (29):4266–74. https://doi.org/10.1016/j.tetlet.2015.05.022.

Wimbiscus, M., O. Kostenko, and D. Malone. 2010. ‘MAO Inhibitors: Risks, Benefits, and Lore’. *Cleveland Clinic Journal of Medicine* 77 (12):859–82. https://doi.org/10.3949/ccjm.77a.09103.

‘World Wide Words: In Silico’. 2006. World Wide Words. 2006. http://www.worldwidewords.org/weirdwords/ww-ins1.htm.

Yamashita, Atsuko, Satinder K. Singh, Toshimitsu Kawate, Yan Jin, and Eric Gouaux. 2005. ‘Crystal Structure of a Bacterial Homologue of Na+/Cl--Dependent Neurotransmitter Transporters’. *Nature* 437 (7056):215–23. https://doi.org/10.1038/nature03978.

7 Appendix

7.1 Extended Data

7.1.1 Stochastic Pocket Script

```
#svl

#set main stochPrep

function stochPrep []

local recatoms = _Atoms '$$receptor';
local residues = uniq aResidue recatoms;
local keepFlexibleRes = [104,335,493,494,501,497,175];

aSetFixed[recatoms,1];
aSetFixed[_Atoms '$$solvent',1];

local m = m_join[rUID residues ,keepFlexibleRes];
local resFlex = residues|m;

aSetFixed[cat (rAtoms resFlex),0];
aSetFixed[Atoms[]|(aBackbone Atoms[],1];

aSetSelected[Atoms[]|(aFixed Atoms[] == 0),1];
endfunction
```

7.1.2 Results of the Binding Energy Calculations in detail

7.1.2.1 Three of the tested Azo-Compounds

Molecule	MM-GBSA ΔG E-config.	Interactions	MM-GBSA ΔG Z-config.	Interactions
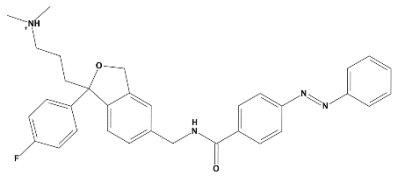 DD-261	-97.364 -94.509	Thr497 π Thr497 Ala500	-111.501 -111.477	No interactions
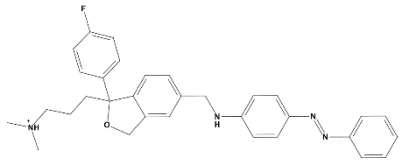 DD-300	-96.716 -79.260		-86.238 -98.639	No interactions
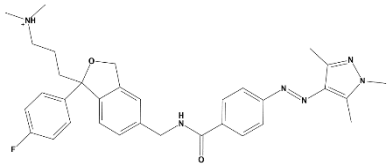 DD-301	-108.923 -108.643		-95.916 -95.389	No interactions

7.1.2.2 The tested HTI-Compounds

Molecule	MM-GBSA ΔG E-config.	Interactions and orientation (AS= allost. binding site)	MM-GBSA ΔG Z-config.	Interactions and orientation (AS= allost. binding site)
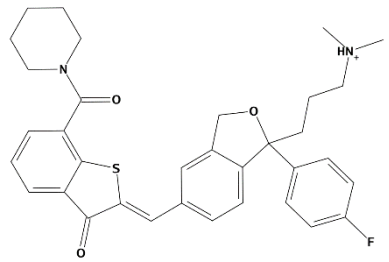 DD-355	-119.398 -119.074 -120.654 -119.150 x=-119.47 v=0.4068 s=0.6378	AS AS AS AS	-108.630 -104.250 -108.903 -110.571 x=-108.09 v=5.4634 s=2.3374	Glu493 Gly498 Gly498, Arg104
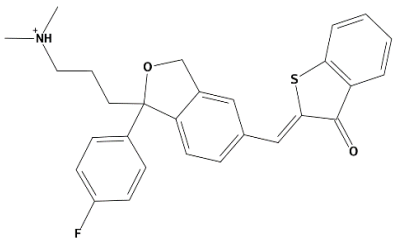 **DD-359**	-106.298 -107.004		**-110.118** -110.118 -108.729	No interactions
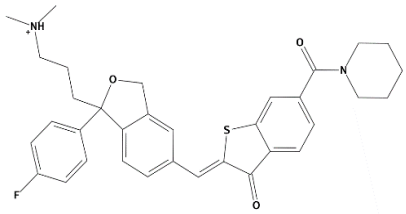 DD-355_m1	**-109.923** -109.349 -112.226	Thr497, AS Thr497, AS Gly498, AS	-105.822 -108.701 -105.266	No interactions

Molecule	MM-GBSA ΔG E-config.	Interactions and orientation (AS= allost. binding site)	MM-GBSA ΔG Z-config.	Interactions and orientation (AS= allost. binding site)
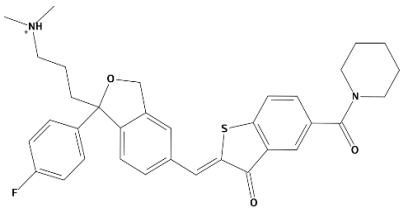 DD-355_p	-108.013 -107.657 -108.009 -107.797 x=-107.869 v=0.0226 s=0.1504	 Arg104 AS π Glu493 Arg104	**-131.079** -130.251 -130.320 -130.191 x=-130.46 v=0.1297 s=0.3601	Tyr175, AS Thr497 -,- -,- -,-
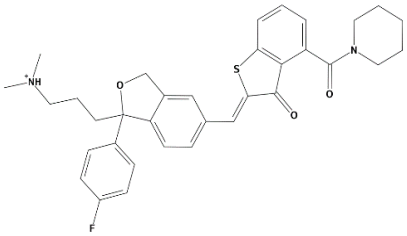 DD-355_m2	-106.009 -110.506	 π Tyr175	-113.970 -115.741	Thr497, AS Glu494 -,-

Molecule	MM-GBSA ΔG E-config.	Interactions and orientation (AS= allost. binding site)	MM-GBSA ΔG Z-config.	Interactions and orientation (AS= allost. binding site)
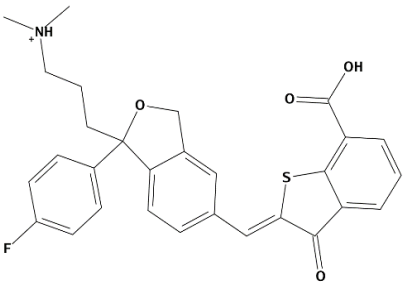 DD-350	-109.698 -110.065 -109.974 -110.017 x=-109.939 v=0.0203 s=0.1425	AS AS AS AS	-109.460 **-118.844** -116.230 -119.029 x=-115.89 v=15.01 s=3.8743	Glu493, AS Thr497 Thr497, AS Thr497, AS Glu493, AS Thr497
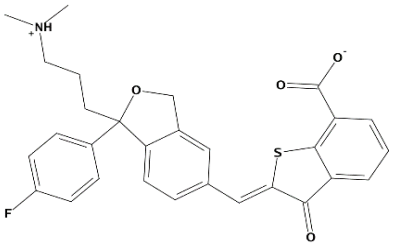 DD-350^{-}	-98.159 -98.284 -95.842 -97.890 x=-97.5438 v=0,9856 s=0.9928	AS AS AS AS	-95.208 **-107.437** -95.974 -100.583 x=-99.801 v=23.6654 s=4.8647	Thr497, AS Thr497, AS Arg104, Na^{+} Thr497, AS Arg104, AS Na^{+}

Molecule	MM-GBSA ΔG E-config.	Interactions and orientation (AS= allost. binding site)	MM-GBSA ΔG Z-config.	Interactions and orientation (AS= allost. binding site)
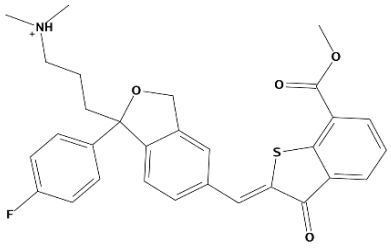 DD-353	-113.469 -115.731 -115.057 -114.532 x=-114.697 v=0.6835 s=0.8267	AS AS AS AS	-103.362 -103.992 -100.605 -102.553 x=-102.96 v=1.6244 s=1.2745	No interactions
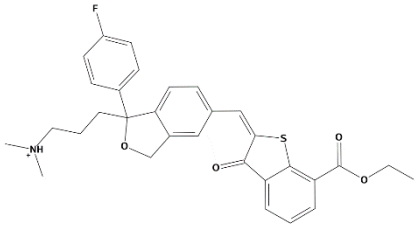 DD-354	-117.535 -117.862 -106.047 -118.448 -105.935 x=-113.165 v=3.4015 s=5.8653	AS AS π Gly497, AS π Phe355 AS π Gly498, AS	-107.954 -119.379 -107.833 -107.038 -99.112 x=-108.26 v=41.8175 s=6.4666	Thr497 Tyr175 Tyr175 Tyr175

Molecule	MM-GBSA ΔG E-config.	Interactions and orientation (AS= allost. binding site)	MM-GBSA ΔG Z-config.	Interactions and orientation (AS= allost. binding site)
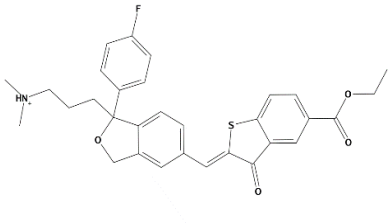 DD-354p	-100.303	Arg104 Tyr175	-119.406	Thr497, AS Tyr175 π Val501
	-97.885	Arg104 Thr497 π Gly498	**-123.055**	-,-
	-98.76	Tyr175	-109.565	Tyr175, AS Thr497, π Ile172
	-99.278	Tyr175 π Gly493 π Ile172	-120.05	Tyr175, AS π Ile172 π Val501
	x=-99.06 v=0.7658 s=0.8751		x=-118.02 v=25.72 s=5.0715	

7.2 Abstract

Until to date, scientists do not yet fully understand the transport mechanism of the human serotonin transporter (hSERT). A big step towards elucidation was made when in April 2016 the crystal structure of hSERT was published. It shows two escitalopram molecules (a commonly prescribed antidepressant), one bound in the central binding site, the other in a new allosteric binding site. These binding sites are separated by a phenylalanine (Phe335) and a tyrosine (Tyr176). The crystal structure gives us an idea how escitalopram molecules could be bound to the transporter molecule. Based on these new findings, novel drugs treating depressive disorders with an escitalopram-like scaffold could be found.

Compounds containing a diazo bond or a hemithioindigo structure (HTI) may switch from E- to Z-configuration (or vice versa) when stimulated with light. This phenomenon is called photoswitch. When adding a photoswitchable substituent to an escitalopram molecule, one of the configurations may fit better into the central binding pocket of hSERT than the other.

This diploma thesis' aim was to investigate the differences in protein-ligand interactions, binding energies and therefore activity values between the E- and Z-configurations of photoswitchable ligands based on an escitalopram scaffold in the central binding site of hSERT on a molecular level. The experiments refer to possible differences in the ligands' physical and chemical properties and interactions with the transporter. To achieve this aim, computational energy calculations and molecular docking studies were performed.

The computational predictions led to the conclusion that some HTI-compounds show the possibility to be used as photoswitchable substituents on escitalopram molecules. These findings could pave the way for design of new drugs for antidepressant therapy.

7.3 Zusammenfassung

Bis heute verstehen Wissenschaftler/innen den Transportmechanismus des humanen Serotonintransporters (hSERT) noch nicht vollständig. Ein großer Beitrag zur Aufklärung ist im April 2016 gelungen, als Coleman et al. die Kristallstruktur von hSERT publiziert haben. Darin sind zwei Moleküle eines häufig verschriebenen Antidepressivums, Escitalopram, gebunden, eines in der zentralen Bindungsstelle, das andere in einer neu entdeckten allosterischen Bindungsstelle. Diese zwei Bindungsstellen sind durch ein Phenylalanin (Phe335) und ein Tyrosin (Tyr176) getrennt. Die Kristallstruktur vermittelt eine Vorstellung davon, wie Escitalopram-Moleküle an das Transporter-Molekül gebunden sein könnten. Aufgrund dieser neuen Ergebnisse können neuartige Escitalopram-ähnliche Wirkstoffe erforscht werden um depressive Erkrankungen zu behandeln.

Moleküle, die eine Diazobindung oder eine Hemithioindigo-Struktur (HTI) besitzen, können bei Stimulation durch Licht von ihrer E-Konfiguration in ihre Z-Konfiguration übergehen oder umgekehrt. Dieses Phänomen wird als Photochromie oder Photoswitch bezeichnet. Wird ein Escitalopram-Molekül mit einem photochromen Strukturelement substituiert, besteht die Wahrscheinlichkeit, dass eine der Konfigurationen besser in die zentrale Bindungstasche von hSERT passt als die andere.

Das Ziel dieser Diplomarbeit besteht darin, die Unterschiede zwischen den E- und Z-Konfigurationen der photochromen, Escitalopram-ähnlichen Liganden anhand ihrer Wechselwirkungen und Bindungsenergie zur zentralen Bindungsstelle von hSERT und die daraus resultierenden Aktivitäten zu erforschen. Die Experimente stützen sich auf mögliche Unterschiede der Liganden bezüglich ihrer physikalischen und chemischen Eigenschaften, sowie ihrer Wechselwirkungen mit dem Transportermolekül. Um das Ziel zu erreichen wurden computergestützte Energieberechnungen und molekulares Docking angewendet.

Die computerbasierten Voraussagen führten zu dem Schluss, dass manche HTI-Strukturen die Möglichkeit zeigen, als photochrome Substituenten an Escitalopram-Molekülen eingesetzt zu werden.

Diese Resultate können den Weg für neue Wirkstoffe in der Therapie mit Antidepressiva ebnen.